Investigating Tropospheric Hydrogen Peroxide Trends from 1950-2014

by

Vanessa Sun

B.A. (Honors), Macaulay Honors College and Hunter College,
City University of New York (2016)

Submitted to the Department of Earth, Atmospheric, and Planetary Sciences,
in partial fulfillment of the requirements for the degree of Master of Science in Earth and Planetary Sciences at the Massachusetts Institute of Technology

May 2024

Authored by: .....
Vanessa Sun
Department of Earth, Atmospheric, and Planetary Sciences
May 23, 2024

Certified by: .....
Arlene Fiore
Peter H. Stone and Paola Malanotte Stone Professor of Earth, Atmospheric and Planetary Sciences
Department of Earth, Atmospheric, and Planetary Sciences,
Thesis supervisor

Accepted by: .....
Robert van der Hilst
Schlumberger Professor of Earth Sciences
Head, Department of Earth, Atmospheric, and Planetary Sciences

Investigating Tropospheric Hydrogen Peroxide Trends from 1950-2014

by

Vanessa Sun

Submitted to the Department of Earth, Atmospheric, and Planetary Sciences,
in partial fulfillment of the requirements for the degree of

Master of Science in Earth and Planetary Sciences

at the

Massachusetts Institute of Technology

May 2024

Abstract

The oxidizing capacity of the atmosphere, or the ability of the atmosphere to clean itself of the pollutants that build up in the troposphere, is determined by oxidants including ozone (O_3), HO_x radicals (OH and HO_2), and hydrogen peroxide (H_2O_2). O_3 is the primary source for HO_x radicals, while H_2O_2 is a key sink for HO_x radicals that terminates the rapid cycling between OH and HO_2. The concentrations of the HO_x radicals and H_2O_2 are difficult to measure directly, with scarce long term data of H_2O_2 primarily available through ice core records. Given the lack of observational data, much of our knowledge on the history of tropospheric oxidants relies on modeling studies. We quantify the global H_2O_2 burden and trends between 1950 and 2014 from the Community Earth System Model - Whole Atmosphere Community Climate Model version 6 (CESM2-WACCM6). This is a global chemistry-climate model, with each of the 13 ensemble members simulating the historical period. Each has a miniscule difference in their initial conditions, and subsequently yield different responses when reacting to the same external forcing. In this study, we discern where H_2O_2 is increasing in the troposphere, particularly in the Southern Hemisphere and over Antarctica. We quantify a rate of increase for the H_2O_2 annual burden, noting the rise beginning in the 1970's and growing from 14% in the 1970's to 34% in the 2000's, with respect to the burden in the 1950's. We find that changes in globally averaged annual mean H_2O_2 are most strongly correlated with changes in ozone, whereas over Antarctica, the strongest relationships for H_2O_2 trends occur with ozone photolysis rates. This aligns well with previous ice core and modelling studies in the literature. Lastly, we also find evidence of stratospheric ozone depletion having no discernible impact on global H_2O_2 burden changes using an additional parallel set of simulations holding ozone depleting substances at 1950 levels.

Thesis Supervisor:	Arlene Fiore
Title:	Peter H. Stone and Paola Malanotte Stone Professor of Earth, Atmospheric and Planetary Sciences
Department:	Department of Earth, Atmospheric, and Planetary Science

Acknowledgements

I would firstly like to acknowledge Arlene Fiore and Qindan Zhu, the primary researchers I worked with on my project. Many thanks to the other members of my thesis committee as well, which includes Jesse Kroll and David McGee. Jesse was particularly influential to my early introduction to atmospheric chemistry as my professor. I loved the class and hope to continue making new atmospheric chemistry discoveries for a long, long time! There are also those in my research group who helped me on technical details of my project, primarily Xinyuan Yu and Steph Elkins.

Next, I would like to acknowledge those at MIT who have supported me, either by just being a friendly face, someone I could talk to, someone I cried to, or made me feel welcome here, including: all of my research group (TEAMPACCC), John Urschel, Ellen, Lesly, Tiange, Diana, Fatima, Timur, Irene, Anthony, Emmie, Olivier, Gareth, Paige, Rina, Manlin, Angie, Ajay, Rikab, and Robert ($\times 2$). Most of all, I am thankful for the people who were there for me through the worst period of it all: James Hall, David Madrigal Trejo, and Fernanda.

Thank you to friends at Harvard, who gave me a place to run away to: Ariana Elena Castillo, Eliel, and Josh Cox. And to the random Chemistry postdoc who stopped to talk to me for over an hour one random day while I cried outside the Infinite. And to Annie, all the OURFA2M2 organizers, Vanessa Maciel, Nicole Mizrahi, Jennifer Wu, and Laura Petto. Thank you to my parents, who gave up a lot for me to be here today, and to my sister—I'm glad you followed me to Cambridge after I followed you to New York City for college.

Thank you, Caroline Draxl, Randye Rutberg, Alicia Prieto Langarica, Adam Sheffer, and Daniel Cruz, for being wonderful mentors, and Emily Franklin and Sarah Benish for helping me apply to the program the first time, but also for helping me when I applied to grad school again. Luckily, I also had Katy Rico and Rebecca Gjini the second time.

I will forever be grateful to everyone I met through the MSRI-UP REU: thank you Team #1 (Fabian and Sam), as well as Alex Barrios, Edray Goins, and William. Lastly, I would not be here today without the MSRI-UP directors, who were the first ones to see my potential to be a researcher and gave me the chance to pursue my dreams.

Table of Contents

1 Motivation

Despite numerous studies on O_3 and OH, few studies focus on quantifying tropospheric H_2O_2 burden change specifically. This thesis focuses aims to to expand knowledge on the changes in H_2O_2 burden in the troposphere including where it has been increasing in recent decades, mechanisms for why its increase, and how this may vary globally versus regionally. In a deviation from the literature, my study focuses on H_2O_2 trends in the time period from 1950 to 2014, rather than comparisons between pre-industrial to present day. These decades have yielded significant global increases in tropospheric ozone, coinciding with increases in emissions of precursors that form ozone such as methane (Hoesly et al. 2018). The largest increases in tropospheric ozone were found to occur after 1950 by Shindell, Faluvegi, Lacis, et al. (2006), thus forming a reasonable starting point for our research. With few modeling studies examining changes in H_2O_2 specifically, we want to understand why the atmospheric burden of H_2O_2 has been increasing globally over time and its spatial distribution. I share our efforts to understand how H_2O_2 has changed over the last few decades by analyzing the trends in the atmospheric burden from the Community Earth System Model-Whole Atmosphere Community Climate Model (CESM2-WACCM6). In the first section discussing our findings, Section 4.1, I determine where tropospheric burden is distributed spatially and quantify the changes globally in separated by the Northern and Southern Hemisphere, noting a greater relative increase in H_2O_2 in the Southern Hemisphere. I discuss the sinks for H_2O_2 in the following section, Section 4.2 and the atmospheric lifetime of H_2O_2 in Section 4.2.2. I relate changes in hydrogen peroxide to changes in its precursors of ozone and OH, along with other species that can contribute to H_2O_2 fluctuations in Section 4.3, noting which chemical species are more strongly related to changes in H_2O_2. Then, I analyze how the ozone photolysis rate relates to H_2O_2 and introduce an additional proxy of $j_{O(^1D)}\times O_3$ to relate to global H_2O_2 in Section 4.4. In Section 4.5, which relies on results from ice core measurements, I establish how the tracers for H_2O_2 change in prior sections have a different relationship with H_2O_2 over Antarctica, especially at the surface level. Lastly, I provide evidence for how stratospheric ozone depletion influences global tropospheric H_2O_2.

2 Introduction

The abundances of several oxidants, termed the oxidizing capacity of the atmosphere, largely determines the removal rates of pollutants from the atmosphere. Key trace gas oxidants that contribute heavily to the oxidizing capacity include ozone (O_3), the hydroxyl radical (OH), and hydrogen peroxide (H_2O_2). As OH reacts with many pollutants, the availability of OH determines the lifetime of many emissions and their products in the troposphere. This has implications for air quality and climate change, as understanding the oxidative capacity of the atmosphere improves understanding of the atmosphere's ability to clean itself of both anthropogenic and natural pollutants including reactive greenhouse gases.

Our primary oxidants are chemically related as follows: OH often reacts in a catalytic cycle with HO_2, and they are often referred to together as the HO_x radicals. Ozone serves as a precursor of OH, while the formation of hydrogen peroxide is a removal mechanism for HO_x from the troposphere. The role of H_2O_2 as a HO_x sink is vital to a complete understanding of

the fluctuations in the troposphere's overall oxidative capacity. There is much to be expanded in the literature on the historical trends for the H_2O_2 oxidant specifically. Accordingly, our research focuses primarily on H_2O_2 and its changes.

2.1 Simplified HO_x Chemistry

In this section, we introduce the basic chemistry to understand how our main oxidants of study (O_3, OH, and H_2O_2) are produced in the troposphere and how they are related to one another. Ozone primarily forms in the troposphere by reaction with hydrocarbons, carbon monoxide (CO), and nitrogen oxides (NO_x), and is also transported from the stratosphere downward into the troposphere (Calvert et al. 2015). Solar radiation of wavelength 240-320 nm dissociates O_3 to excited states of O and O_2 (Seinfeld and Pandis 2016), as shown in Reaction 1.

$$O_3 + h\nu \longrightarrow O(^1D) + O_2 \tag{1}$$

When $O(^1D)$ collides with water vapor, it forms two OH radicals. This is described by Reaction 2:

$$O(^1D) + H_2O \longrightarrow 2\,OH \tag{2}$$

The OH radical frequently reacts with CO to form CO_2 and hydrogen, with the hydrogen atom quickly reacting with O_2 to form HO_2, the hydroperoxyl radical, HO_2, and carbon dioxide, CO_2. These reactions are described in the shortened form by Reaction 3.

$$CO + OH \xrightarrow{O_2} CO_2 + HO_2 \tag{3}$$

In the presence of NO_x, HO_2 reacts with NO to form NO_2 and OH, as in Reaction 4 (Seinfeld and Pandis 2016):

$$HO_2 + NO \longrightarrow NO_2 + OH \tag{4}$$

Then, given sufficient NO concentrations of 20 ppt, there is a rapid cycling that can occur between OH and HO_2, where Reaction 3 generates HO_2 that converts back to OH with Reaction 4 (Calvert et al. 2015). The OH and NO_2 products can react to form nitric acid, HNO_3, which removes HO_x and NO_x radicals as described by Reaction 5:

$$OH + NO_2 + M \longrightarrow HNO_3 + M \tag{5}$$

In the remote troposphere, where NO concentrations are often below 20 ppt, HO_2 will not always react with NO, as described by Reaction 4(Calvert et al. 2015). Instead, the following HO_2 reactions are dominant and compete for HO_2 (Calvert et al. 2015):

$$HO_2 + HO_2 \longrightarrow H_2O_2 + O_2 \tag{6}$$

$$HO_2 + RO_2 \longrightarrow ROOH + O_2 \tag{7}$$

with alkyl peroxy radicals denoted by RO_2 and hydroperoxides denoted by ROOH (Seinfeld and Pandis 2016). Reaction 6 describes the formation of hydrogen peroxide, H_2O_2, in the troposphere. After H_2O_2 is produced, the main loss process for H_2O_2 is by dry and wet

deposition, bringing reaction products to the surface and removing HO_x radicals from continued interaction in the troposphere (Murray et al. 2014). This thesis work largely focuses on the H_2O_2 loss from deposition as the primary hydrogen peroxide sink. However, H_2O_2 is not always lost by this physical process. H_2O_2 can also act as a reservoir species for HO_x by photolyzing, and reaction with OH, as in (Seinfeld and Pandis 2016):

$$H_2O_2 + h\nu \longrightarrow OH + OH \tag{8}$$

$$H_2O_2 + OH \longrightarrow HO_2 + H_2O \tag{9}$$

I neglected to include the role of these additional sinks in balancing the H_2O_2 budget in my analysis, focusing on the main depositional loss processes. The limitations of this simplification and potential avenues to incorporate the role of Reactions 8 and 9 are described in Section 4.2.3.

A summary of the main reactions in this section, describing the basic pathways to create and remove HO_x in the troposphere, is provided in a diagram in Figure 1 below.

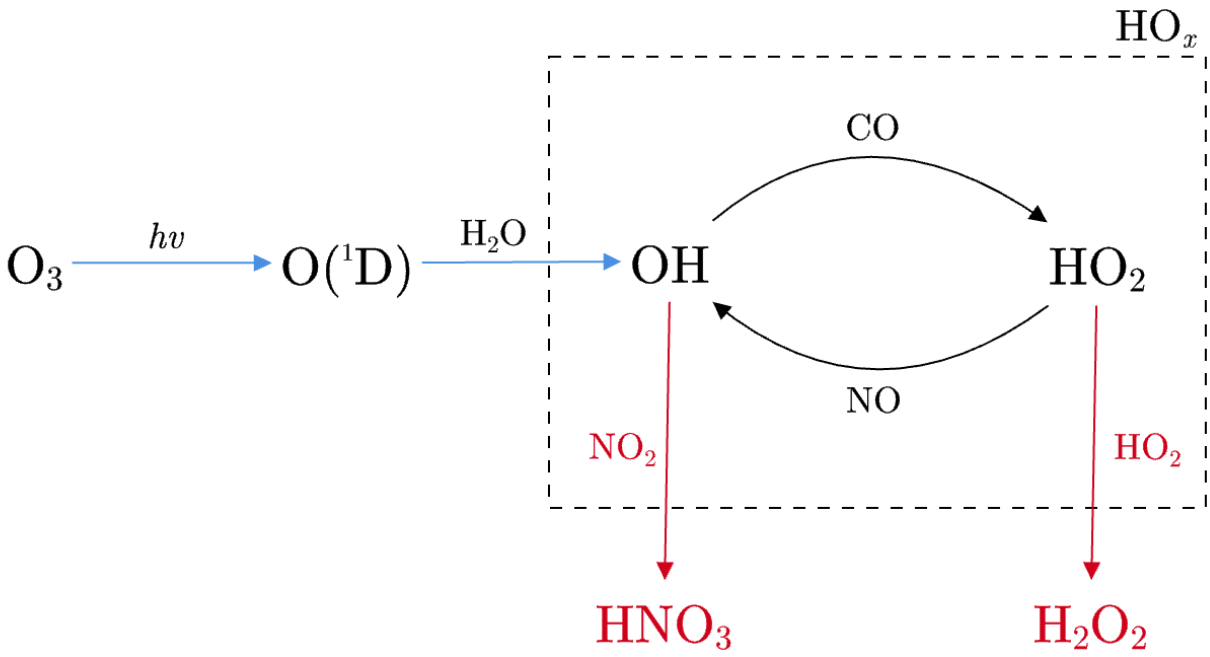

Figure 1: Diagram of chemical reactions relating to the formation and removal of HO_x in the troposphere. The blue represents the sources of HO_x and red represents the sinks.

2.2 Current knowledge of tropospheric H_2O_2

2.2.1 Observational studies

Much of the focus in the literature on our key oxidants has been centered on identifying trends over time in ozone and OH. There is general acceptance of ozone increasing over time in surface ozone in observational studies, with not much change from the late 1800's to around 1975, and large increases in remote and rural surface ozone from 1975 to the present day (Tarasick et al. 2019). Increases of ozone have also been measured in the free troposphere (Tarasick et al. 2019). Through ice cores, proxies can help estimate OH and O_3 change over longer time scales, prior to the pre-industrial era (Alexander and Mickley 2015; Sofen, Alexander, Steig, et al. 2014; Gillett et al. 2000). In this section, I provide an overview of what is available in the literature regarding hydrogen peroxide trends, supported by observational studies including rainwater, aqueous phase, gas-phase, precipitating snow, surface snow, snow pit, hoarfrost, firn, and ice core measurements. The main findings are:

1. Typical surface level and near-surface volume mixing ratios for H_2O_2, and some measurements at higher tropospheric altitudes
2. Greater H_2O_2 concentrations in Greenland than Antarctica
3. Clear seasonality in H_2O_2
4. Observed increases in H_2O_2 in recent decades
5. Some evidence of stratospheric ozone depletion motivating the increases in H_2O_2, along with tropospheric chemistry changes.

Sparse and short-term gas-phase measurements of surface and near-surface H_2O_2 have been taken since the 1990's. The measurements can be compared to our own model estimates and ensures that we have reasonable surface H_2O_2 concentrations for the nearby areas. The first gas-phase H_2O_2 measured in Greenland yielded a range of 300-3500 ppt during June/July 1990 (Sigg, Staffelbach, and Neftel 1992). Later measurements include a mean volume mixing ratio of 1000 ppt in May/June 1993 (Bales et al. 1995) and 650 ppt in June/July 2000 (Jacobi et al. 2002). In Antarctica, the first gaseous H_2O_2 measurements were conducted by Jacob and Klockow 1993 in December 1989/January 1990, where a mean H_2O_2 concentration of 394 ppt was observed. Other studies showed around 200-300 ppt in summer 1994 and between 1997 and 2000 (McConnell et al. 1997; Riedel et al. 2000; Hutterli, McConnell, Chen, et al. 2004), and 90-100 ppt in 1996 (McConnell et al. 1997). For 2000-2002, Frey, Stewart, et al. (2005) measured H_2O_2 concentrations of 321 $\pm$ 158 ppt, 650 $\pm$ 176 ppt, and 330 $\pm$ 147 ppt in December.

The gas-phase measurements also indicate that the surface concentration of H_2O_2 in Greenland is greater than the Antarctic H_2O_2 concentration. However, these observations are sparse and provide short-term data that are sensitive to varying meteorological conditions that may alter their concentrations quickly. This highlights the need for a longer term, consistent tracer of hydrogen peroxide, especially to understand H_2O_2 on a global scale, which is available primarily through ice cores records. Ice cores hold the only centuries-long, historical records of H_2O_2 change, allowing us to understand the changes between the

Last Glacial Maximum, pre-industrial, and present day tropospheric burdens. Comparing H_2O_2 from cores taken in both Greenland and Antarctica, the earliest ice cores analyzed by Neftel, Jacob, and Klockow 1984 found significantly more H_2O_2 in the Greenland cores than Antarctic ones. This shows that the Greenland H_2O_2 concentrations were higher over a much longer time period, and not solely in the present day.

Neftel, Jacob, and Klockow (1984) also found a strong seasonal variation, with higher H_2O_2 concentrations in summer and lower H_2O_2 in winter. Seasonal trends were affirmed in additional Antarctic ice cores taken by Gillett et al. (2000), firn and ice core measurements for both Greenland and Antarctica in Sigg and Neftel (1988), and surface snow measurements from McConnell et al. 1997. This seasonality is also supported by rainwater (Bufalini et al. 1979; Kok 1980) and aqueous-phase measurements (Kelly, Daum, and Schwartz 1985). However, in other observations, there was a weakening or lack of seasonal trend. Sigg, Staffelbach, and Neftel 1992 found in Greenland firns that the seasonality started to weaken with increasing depth and even disappears after the transition from firn to ice. In Antarctic firn measurements below 2m and pit measurements by Jacob and Klockow (1993), there were no seasonal H_2O_2 trends detected. Sigg, Staffelbach, and Neftel (1992) identifies differences in accumulations as the likely cause for the lack of H_2O_2 preservation in snow and ice. After conducting snow pit and ice core studies in Antarctica, Frey, Bales, and McConnell (2006) emphasized that areas of high accumulation and low temperatures create the best conditions for H_2O_2 preservation. This emphasizes a potential limitation in using these measurements. In some areas of Antarctica, such as the WAIS Divide, it can be difficult to estimate accumulations of the past, due to inconsistencies in the relationship between the accumulation record and the Antarctic Oscillation (Banta et al. 2008). A similar physical process, snow formation, is also identified as a potential cause of the inconsistencies between Greenland and Antarctic ice core H_2O_2 concentrations in Neftel, Jacob, and Klockow (1984).

In the last few centuries, there is a clear trend of increases in H_2O_2, found in both Greenland and Antarctic ice cores. Two key studies of Greenland ice cores estimated an increase of 50% over the last 200 years (Sigg and Neftel 1991) and a quantified increase of $60 \pm 12\%$ in the last 150 years (Anklin and Bales 1997). In Antarctica, Gillett et al. (2000) found pre-industrial H_2O_2 concentrations of 1.0μ mol L^{-1} to 1.2μmol L^{-1} in their ice cores and present day concentrations of 1.6μ mol L^{-1} to 2.1μ mol L^{-1}, indicating an increase over the past few centuries. Further ice core studies constrain the more recent increases, attempting to identify a time period that the most significant changes occurred. In 23 ice cores drilled across Antarctica, Frey, Bales, and McConnell (2006) reported a large increase in H_2O_2 concentrations starting in the late 1950's or later, apparent in all cores. Sigg and Neftel (1991) suggests 1960 to 1988 as a time period of H_2O_2 increase.

A commonly suggested mechanism in the literature for the H_2O_2 increase in recent decades is the stratospheric ozone depletion across the 1980's and 1990's. Frey, Stewart, et al. (2005) identifies a negative correlation between surface stratospheric O_3 and H_2O_2 in Antarctic gas-phase measurements. However, a conflicting result from Riedel et al. (2000) found that gas-phase H_2O_2 measurements taken during the stratospheric ozone depletion periods were no different from the typical winter concentrations. Anklin and Bales (1997) identifies that increased UV-B radiation stimulating the photolysis of ozone to OH and therefore increasing H_2O_2 is not the only process that increases H_2O_2. They suggest changes in tropospheric chemistry have to also be accounted for in driving tropospheric H_2O_2.

2.2.2 Modeling studies

Modeling studies that explore changes from tropospheric pre-industrial H_2O_2 to present day H_2O_2 are slightly more plentiful in the literature. The change between the pre-industrial H_2O_2 to present day H_2O_2 burden relative to pre-industrial levels spans a large range, from 31% in Murray et al. 2014 to 100% in Berntsen et al. 1997 (Murray et al. 2014; Grenfell et al. 2001; Sofen, Alexander, and Kunasek 2011; Berntsen et al. 1997). Berntsen et al. 1997 and Grenfell et al. 2001 also quantify changes in the Northern and Southern Hemisphere separately. These values are all summarized in Table 1. From these studies, we see an overall global increase in H_2O_2 from the pre-industrial era to the present day. Over Greenland, the change in tropospheric H_2O_2 burden was quantified as a 44% increase when comparing the pre-industrial to present day change at 3 km in Martinerie, Brasseur, and Granier 1995, while Wang and Jacob 1998 stated a 2.5 factor increase. Sofen, Alexander, and Kunasek 2011 quantified a global tropospheric mean increase of 58% from the pre-industrial to the present day, with a spatial map suggesting a maximum increase of around 600 ppt change over Antarctica.

Reference	Global Change	NH Change	SH Change
Berntsen et al. (1997)	100%	117%	80%
Grenfell et al. (2001)	88%	101%	75%
Sofen et al. (2011)	58%	65% ± 3%*	-
Murray et al. (2014)	31%	-	-

* For surface to 8.1 km altitude

Table 1: Relative changes in H_2O_2 tropospheric mean from pre-industrial to present in the literature

3 Methods

The model used for our analysis was the Community Earth System Model-Whole Atmosphere Community Climate Model (CESM2-WACCM6). CESM2 is an Earth system model that describes how different aspects of the Earth system, such as the land, sea ice, ocean (etc.), interact. CESM2 can be configured to run with different component models, including WACCM6 as the atmospheric model, to create coupled simulations (Danabasoglu et al. 2020). WACCM6 provides the atmospheric chemistry representing the troposphere, stratosphere, mesosphere, and lower thermosphere (Emmons et al. 2020).

For our initial condition ensemble, we used three ensemble members that were launched from a long pre-industrial control simulation then extended following historical emissions and forcing trajectories until 2014 (Danabasoglu et al. 2020). To create additional ensemble members, January 1, 1950 was selected to use for initial conditions, each with a small change in atmospheric temperature. Each of the 13 individual ensemble members that have unique possibilities for atmospheric chemistry when subject to the same forcings. The historical

runs were described in Hancock et al. (2023) and Fiore et al. (2022), with an additional ensemble member added since those studies. Throughout our analysis, we mainly use the mean over all 13 ensembles to average out noise and estimate the forced response, or the signal from anthropogenic influence. The range across the ensemble members indicate the uncertainty due to internal climate variability.

Our model output is formatted as large monthly and yearly netCDF files for each ensemble member. The H_2O_2 variable was only saved as a mass mixing ratio in the yearly files, while all other values were saved on monthly files, with various chemical species (O_3, CO, HO_2, NO, etc.) available as volume mixing ratios. Each variable was saved out for 70 vertical levels, with the highest layer representing the surface level. Spatial resolution of WACCM6 is 0.96° latitude ×1.25° longitude. For all relevant cases, a mask was applied to nullify the irrelevant stratospheric values above the tropopause (available as its own variable). Burdens of each chemical species are calculated as a column-sum and summed over the area, with the $j_{O(^1D)} \times O_3$ burden values also following the same procedure. The global $j_{O(^1D)}$ is calculated by taking a pressure-weighted column average and averaging over the area-weighted grid. For the values over a single grid cell in the Antarctica case, H_2O_2 and O_3 are instead represented as volume mixing ratios at surface level. To obtain $j_{O(^1D)} \times O_3$, I multiplied the photolysis rate coefficient at surface level for the grid cell times the volume mixing ratio of O_3 at surface level. The OH values used throughout this thesis are expressed as a concentration, which is more typically used in the literature than a tropospheric burden. These were obtained by Qindan Zhu and describe the number density for OH below the 46^{th} vertical layer to remove stratospheric data.

4 Analysis of CESM2-WACCM6 H_2O_2 Simulations

4.1 Global Distribution and Trends of H_2O_2 Burden

The model I used for my study predicts that globally, H_2O_2 has increased over our time period of interest. The time series plot in Figure 2 shows the estimated H_2O_2 burden in Tg units. Our suggested tropospheric H_2O_2 burden is lower overall than the few existing modeling studies estimating a present-day H_2O_2 atmospheric burden Koch et al. (1999) estimate a burden of 4.2 Tg in their study. In Shindell, Grenfell, et al. (2001), they obtain a burden of 6.4 Tg, but notes an overestimate of H_2O_2 near the equator. Using the GISS ModelE GCM, Murray et al. (2014) estimates 3.4 Tg, and 4.1 Tg for GEOS-CHEM. Our tropospheric H_2O_2 burden values never exceed 3.0 Tg. The difference in the previous studies from our estimates may be due to improved representation of reactions involving organic species in our model. Further study is necessary to evaluate our model's comparison to the previous studies.

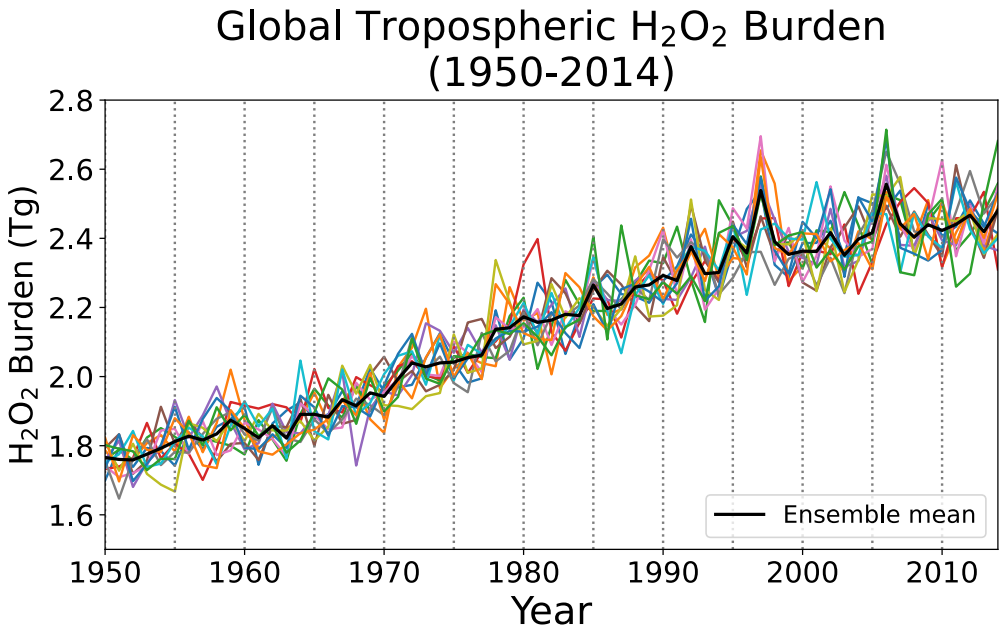

Figure 2: Global tropospheric H_2O_2 burden from 1950 to 2014. Each colored line represents an individual ensemble member, with the black line representing the mean over all 13 ensembles.

The spatial distribution of the annual tropospheric H_2O_2 burden for the time period from 1950 to 1959 is shown in Figure 3. The map shows higher burdens over Central and Western Africa, off the northwest coast of South America, over India, and between Australia and Indonesia. The maximum burden is less than 400 Mg. Over the decades following 1950, the spatial distribution does not change heavily, so that the areas of higher burden are close to what is pictured in Figure 3. This means that the H_2O_2 burden is roughly focused on the tropical region between 30°N and 45 °S latitude.

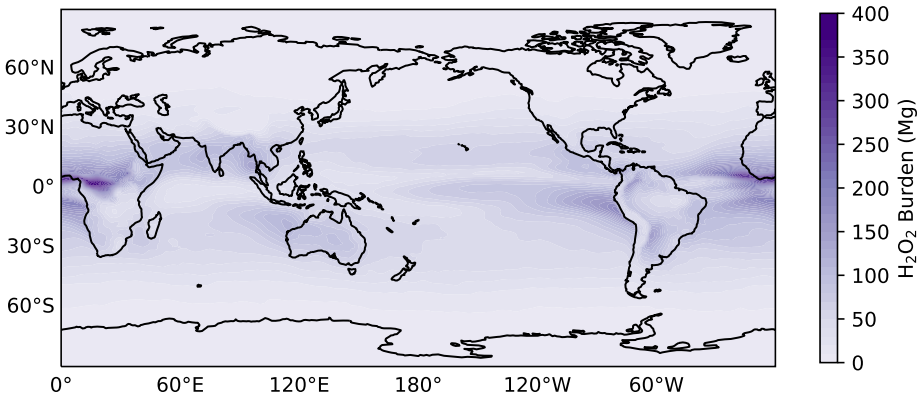

Figure 3: Annual tropospheric H_2O_2 burden for the decade from 1950 to 1959

We note a distinct band of lower H_2O_2 burden near the equator, which follows the intertropical convergence zone (*Inter-Tropical Convergence Zone — National Oceanic and*

Atmospheric Administration 2024). To further investigate why the burden might be lower in this area, we analyze the distribution of H_2O_2 across the upper, middle, and lower troposphere. In Figure 4, we show the respective contributions that the upper, middle, and lower tropospheric H_2O_2 make to the overall H_2O_2 tropospheric burden from 1950 to 1959. With a total global, annual tropospheric burden of 1.80 Tg (or 1800 Gg) for 1950 to 1959, around 710 Gg are located in the lower troposphere, 750 Gg are located in the middle troposphere, and 340 Gg are located in the upper troposphere. Thus, most of the H_2O_2 in the troposphere is located in the middle and lower troposphere. However, the band of lower overall H_2O_2 burden is mostly composed of upper and middle tropospheric H_2O_2, and there is little H_2O_2 in the lower troposphere, as evidenced by their respective percentage contributions in the Figure 4. This is likely due to the increase in precipitation and convective storms that occur in the ITCZ (*Inter-Tropical Convergence Zone — National Oceanic and Atmospheric Administration* 2024), which would remove the H_2O_2 by wet deposition in the lower parts of the troposphere at the narrow band.

In Table 2, we quantify the H_2O_2 burden and change in H_2O_2 burden for each decade compared to the 1950 to 1959 burden. A minor increase of 4.5% H_2O_2 occurs in the 1960's, but this jumps to 14% in the 1970's. Larger increases occur in the 1980's and 1990's, before a smaller increase in the early 2000's. Therefore, most of the burden increase is occurring in the 1970's through the 1990's. Both the overall burden and absolute change in burden in the Northern Hemisphere are higher across all decades, but the relative change is larger in the Southern Hemisphere. The higher abundance in H_2O_2 in the Northern Hemisphere rather than the Southern Hemisphere matches ice core observations from Neftel, Jacob, and Klockow 1984.

Decade	Total Burden (Gg)			Absolute Change (Gg)			Relative Change		
	NH	SH	Global	NH	SH	Global	NH	SH	Global
1950's	980	820	1800	–	–	–	–	–	–
1960's	1080	860	1880	40	40	80	3.9%	5.1%	4.5%
1970's	1110	940	2050	120	120	250	12.4%	15.2%	13.6%
1980's	1200	1020	2210	210	200	400	21.0%	24.0%	22.4%
1990's	1270	1090	2360	290	270	560	29.7%	32.5%	30.0%
2000's	1310	1100	2420	330	280	610	33.6%	34.5%	34.0%

Table 2: Annual H_2O_2 burden and change in H_2O_2 burden per decade, compared to 1950 to 1959 burdens (listed for the 1950s). Each decade represents 10 years; for example, 1960s means the annual burden from 1960 to 1969.

We can analyze the areas where the H_2O_2 burden increases the most through spatial maps. In Figure 5, we see the spatial distribution of the relative change in H_2O_2 annual burden compared to the decade from 1950 to 1959. The plots span select decades: the 1960's, 1980's, and 2000's. From these plots, we see that the H_2O_2 burden has been increasing over time, as expected, with not much change in the earlier decades (1960's) but more significant

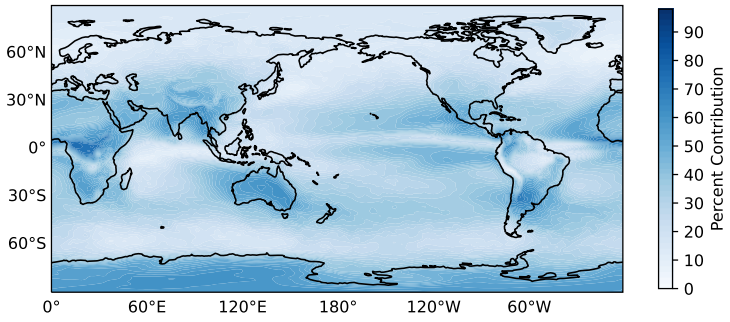

(a) Lower Troposphere

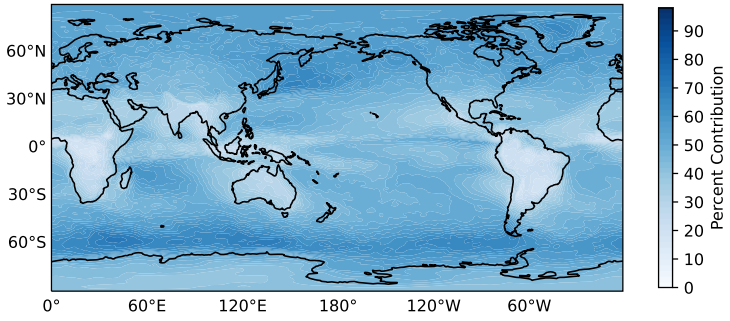

(b) Middle Troposphere

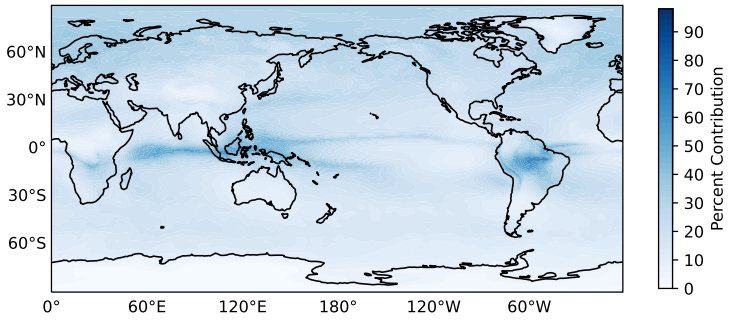

(c) Upper Troposphere

Figure 4: Annual tropospheric H_2O_2 burden for the decade 1950 to 1959, split into the percentage that the upper, middle, and lower tropospheric H_2O_2 contribute to the overall burden

change in the later decades. The areas of highest relative burden increase are over the Indian Ocean, Indonesia, between 35°and 55°S latitude, and over Antarctica. It is clear that the large relative increases in H_2O_2 is larger in the Southern Hemisphere when observing the increases between 35°and 55°S latitude and Antarctica in these spatial plots.

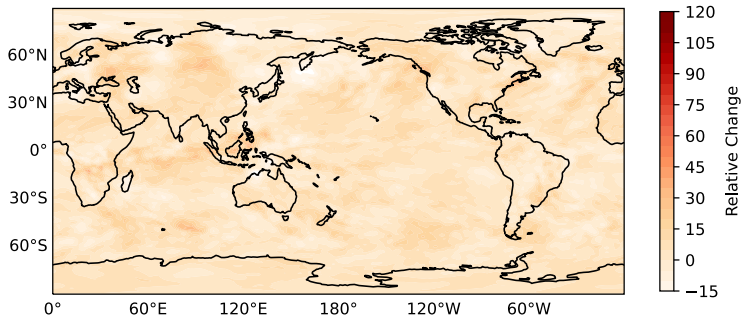

(a) 1960s

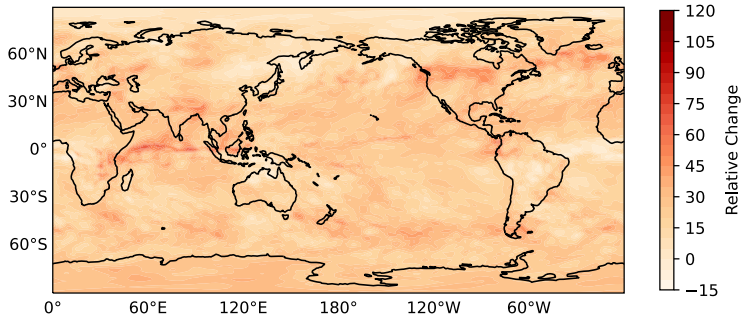

(b) 1980s

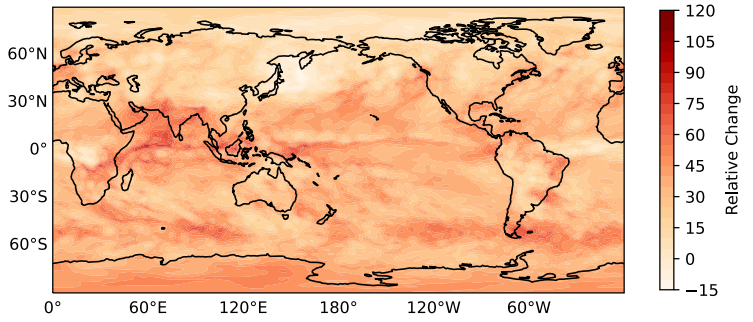

(c) 2000s

Figure 5: Relative change in annual mean H_2O_2 burden for several decades, compared to 1950 to 1959.

4.2 Deposition Rate Analysis and Atmospheric Lifetime

4.2.1 H_2O_2 Loss by Depositional Processes

Now that we have characterized how the H_2O_2 burden is changing in the atmosphere, we can study the processes that control how much H_2O_2 is being added or removed from the atmosphere. A major sink for H_2O_2 from the troposphere for much of the Earth is by deposition, both dry and wet, with these physical loss processes as the largest contributors to overall H_2O_2 loss in the troposphere (Murray et al. 2014). In Figure 6, we have our modeled mean deposition rate for the decade from 1950 to 1959 in units of Gg per year. The spatial distribution of the deposition rate is similar to the spatial distribution of the tropospheric

H_2O_2 burden in Figure 3. This is because deposition is a first order loss rate process, where areas of high H_2O_2 in the troposphere also show higher rates of deposition, as there is more H_2O_2 available to deposit (Seinfeld and Pandis 2016). The areas of higher H_2O_2 deposition in our figure are also in the places that experience heavy rainfall, such as in Central Africa (Masih et al. 2014), as the increased precipitation would remove H_2O_2 by wet deposition. In this section, we look at how the global deposition rate of H_2O_2 has changed over time. We also use the deposition rate to estimate a lifetime for H_2O_2, or how long the chemical stays in the troposphere.

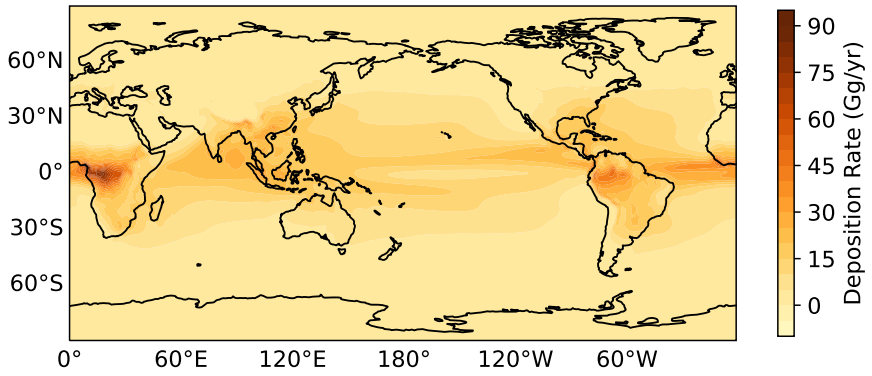

Figure 6: Spatial distribution of H_2O_2 deposition rate from wet and dry deposition combined, for 1950 to 1959.

Over time, the deposition rate of H_2O_2 has increased, as shown in the time series plot of Figure 7. While the graph only displays the combined deposition rate, I created the same type of plot and found that the trends for the individual depositional processes are very similar in both wet and dry deposition in our model, with a larger contribution from the wet deposition. In Figure 7, there is consistency with the time series plot of the H_2O_2 burden in Figure 2. For example, the characteristic sharp increases across the 1990's are a feature of both plots.

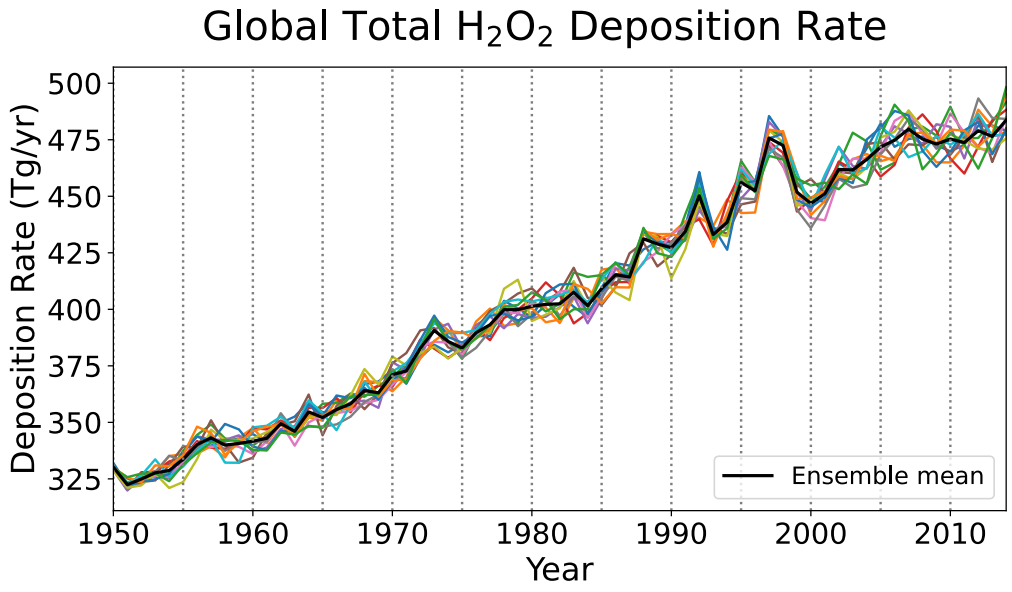

Figure 7: Total global deposition rate of H_2O_2 for 1950 to 2014.

4.2.2 Atmospheric Lifetime with Respect to Depositional Removal Processes

Looking at the deposition rate also helps us to understand how quickly H_2O_2 can be removed from the atmosphere. The lifetime of H_2O_2, or how long it remains in the atmosphere before chemical or physical removal, can be estimated by the relationship:

$$\tau = \frac{\text{Total mass of species}}{\text{Loss of species}}$$

where τ is the atmospheric lifetime (The Intergovernmental Panel on Climate Change 2024). From our model data, the total mass of species is the H_2O_2 burden, while the loss of species is the rate of the depositional loss process. The mean atmospheric lifetime of H_2O_2 against total depositional processes for the areas above 60°S latitude is 4.1 days for wet deposition, 15.7 days for dry deposition, and 2.8 days for total deposition. A shorter lifetime of H_2O_2 against wet deposition indicates that wet deposition is a far more effective removal process for H_2O_2 in the troposphere than dry deposition. We also note other areas where the lifetime is high, including over 12 days around areas of extreme drought in Northern Africa, as the dry deposition removal process is slower (Masih et al. 2014).

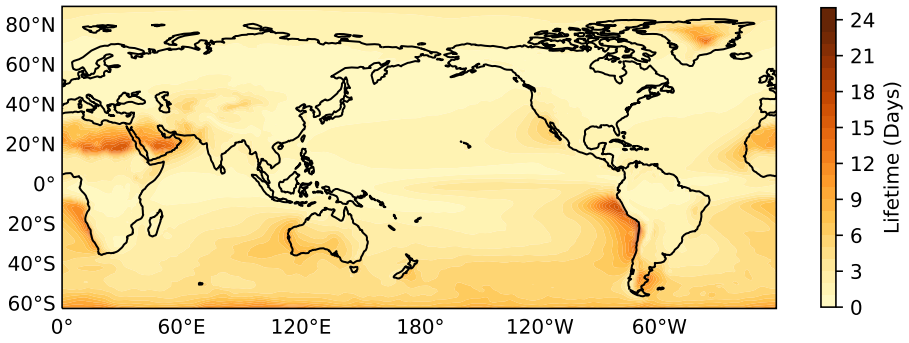

Figure 8: Ensemble and annual mean atmospheric lifetime of H_2O_2 against total deposition (combining dry and wet deposition) in the troposphere, over our entire time period from 1950 to 2014.

For this figure, I chose to focus on the area north of 60°S latitude due to limitations in our model. The chosen area represents the majority of the world but excludes Antarctica, as high atmospheric lifetimes over Antarctica heavily skew the estimates, due to extremely low depositional rates for H_2O_2 over the continent. These depositional loss processes are a main tropospheric sink of H_2O_2 in the polluted boundary layer, where Kleinman (1986) suggests a lifetime of approximately one day. Our spatial map of the H_2O_2 atmospheric lifetime matches closely with this lifetime in the areas where emissions are high. The majority of the troposphere shows a lifetime of only a few days against wet and dry deposition. I also found that the lifetime of H_2O_2 changed very little for most of the Earth over our time period.

4.2.3 Other Loss Processes and Their Contributions to H_2O_2 Lifetime

My initial focus in estimating H_2O_2 lifetimes was on the wet and dry depositional loss processes. However, there are other reactions that tropospheric H_2O_2 undergoes that do not remove H_2O_2 or HO_x immediately from the troposphere. In this section, we discuss where these loss reactions are most prevalent and their potential impacts on the H_2O_2 and HO_x budget.

Riedel et al. (2000) defines the three main loss processes for H_2O_2 in the troposphere: deposition, photolysis, and reaction with OH. All three are used to calculate an overall H_2O_2 lifetime. We have already looked at the loss by deposition more closely in the previous subsection. In the literature, studies have estimated a lifetime of 30 hours for mid-latitudes (Kleinman 1986) and a global lifetime of 28 and 32 hours in two different models (Murray et al. 2014). Over Antarctica, this can be calculated by (Riedel et al. 2000):

$$\tau = (k_{\text{deposition}} + k_{H_2O_2+OH}[\text{OH}] + j_{H_2O_2+h\nu})^{-1}$$

for the lifetime τ during the polar day time. They estimate a H_2O_2 lifetime of around 3 days. In polar regions, dry deposition and H_2O_2 photolysis are not major loss processes. This means that overall lifetimes can be higher in these areas. In the future, we can use this relationship to improve our lifetime estimates, considering the two other major loss processes we neglected in our earlier analysis.

Reaction 8, the photolysis of H_2O_2, generates two OH radicals, affecting the OH budget as a source. It is unclear how often H_2O_2 photolyzes in comparison to other processes, but we can theorize a few trends. Firstly, we expect that this loss process is more prevalent in regions of high photochemical actively. This is mainly in the tropical areas, between around 20°N to the equator and 20 °S to the equator. These are also regions where H_2O_2 burden is also higher, as shown in Figure 3. We may also expect the H_2O_2 photolysis reaction contributes more heavily to OH production at high altitudes than the $O(^1D)$ reaction with water vapor, as there is less water vapor at higher altitudes (Lee, Heikes, and O'Sullivan 2000). If we assume similar mechanisms for H_2O_2 photolysis as O_3 photolysis, the rate of H_2O_2 photolysis would likely increase over our time period, as our $j_{O(^1D)}$ has shown to be increasing throughout this thesis. This would translate to Reaction 8 becoming an increasing sink for H_2O_2, less H_2O_2 lost by depositional processes, and an increasing source for OH. A shortening lifetime from 1950 to 2014 for H_2O_2 with respect to photolysis loss would also be expected, with a faster $j_{H_2O_2+h\nu}$ rate. Our hypothesis of an increasing H_2O_2 photolysis rate can be verified through additional simulations, as although we did not download the variable for $j_{H_2O_2+h\nu}$ in our simulations initially, the H_2O_2 photolysis rate is available in the MOZART chemistry mechanisms for CESM2 (Emmons et al. 2020). Adapted from results of Murray et al. (2014), Seinfeld and Pandis (2016) lists Reaction 8 as a significant OH source, accounting for approximately 11% of the present day OH budget.

For Reaction 9, one OH is consumed, thus it serves as an OH sink. With many other chemical species available for reaction in OH, I speculate that this reaction may not be the most significant OH sink, although it does play a role in modulating the OH and H_2O_2 budgets. With OH budget adapted from Beerling et al. (2011), Seinfeld and Pandis (2016) suggests that Reaction 9 contributes to around 4% of the OH loss in the pre-industrial time period, but it is not mentioned as a significant OH loss process for OH in the present-day. The reaction may potentially contribute around a similar loss of OH in the present day. Since both OH and H_2O_2 burden are increasing over our time period, as shown throughout our analysis, Reaction 9 may be occurring more frequently over time. However, it is unclear how we may be able to understand the impact of this particular reaction further with our current simulations.

4.3 Drivers of Global H_2O_2 Change: Comparing H_2O_2 Burden with O_3 and OH

The modeled changes in burden over time are shown in Figure 9, with each oxidant represented by a different subplot. A closer numerical view of how the oxidant burdens changed by decade are included in Table 3. We can see that all the burdens of all the oxidants generally increased when comparing to the initial decade of 1950 to 1959, but all at different rates. This suggests that each oxidant has its own complex controls that govern their changes, even though the oxidant species are interconnected. Our analysis begins with time series analysis plots, where we see differences in the spread of the ensemble members for each chemical species and can easily compare year-to-year variability between species. With scatterplots of the ensemble mean burdens between two specific species, we can better understand how well correlated a precursor is with its eventual product.

For the ozone burden, depicted in Figure 9a, we observe a gradual increase before 1970. As summarized in Table 3, there is only an increase of 5.04% of the total O_3 burden from the 1960's. This jumps by over 8% in the 1970's, to 14% overall relative increase starting in the 1970's. After 1970, there is more variability in the tropospheric burden, with more frequent increases and decreases shown in the time series plot. There are extended periods of decrease in the early to mid 1980's and 1990's, as well as steep increases from 1992 to 1997. These average out to a small relative increase in O_3 burden of 3.2% in the 1980's and a larger increase of 5.8% in the 1990's. Finally, the burden increases by 8.1% from 2000 to 2009, reflecting an extended period of increasing ozone burden. Overall, the burden never decreases below the 1950 levels. We also note that the spread in the ensemble members is much closer in the ozone burden than for the other oxidants, which may suggest a higher degree of accuracy in these modeled values than for OH and H_2O_2.

In Figure 9b, we observe that OH changes very slightly before 1980, whereas O_3 and H_2O_2 show general increases. The relative changes summarized in Table 3 quantify a decadal increase of only 0.74% for the 1960's and 1.20% for the 1970's, when compared to 1950 to 1959 values. With a significant reduction in OH in the 1982, the 1980's averaged only an increase of 0.20% in decadal OH burden. From the 1990's forward, we observe a general distinct steeper increase in the time series plot and the OH burden increases to its highest point in the late 2000's. These are quantified as a relative change of 4.45% in the 1990's and 10.11% in the 2000's, as compared to 1950 to 1959 burdens. As the OH burden does not follow the same continuous upward trend as ozone, it is likely that changes in sinks for OH depressed the burden in the earlier years. The sudden increase in OH after 1990 may be associated with increased conversion of ozone to OH, which we explore more in depth in further sections. The NO burden depicted in Figure 9c shows a general increase until 1980, where it decreases in 1980 before recovering in the late 1980's. Comparing to OH, NO was increasing prior to the 1980's, while OH was mostly stagnated. This changes from 1980 forward, where we see close agreement between NO and OH trends.

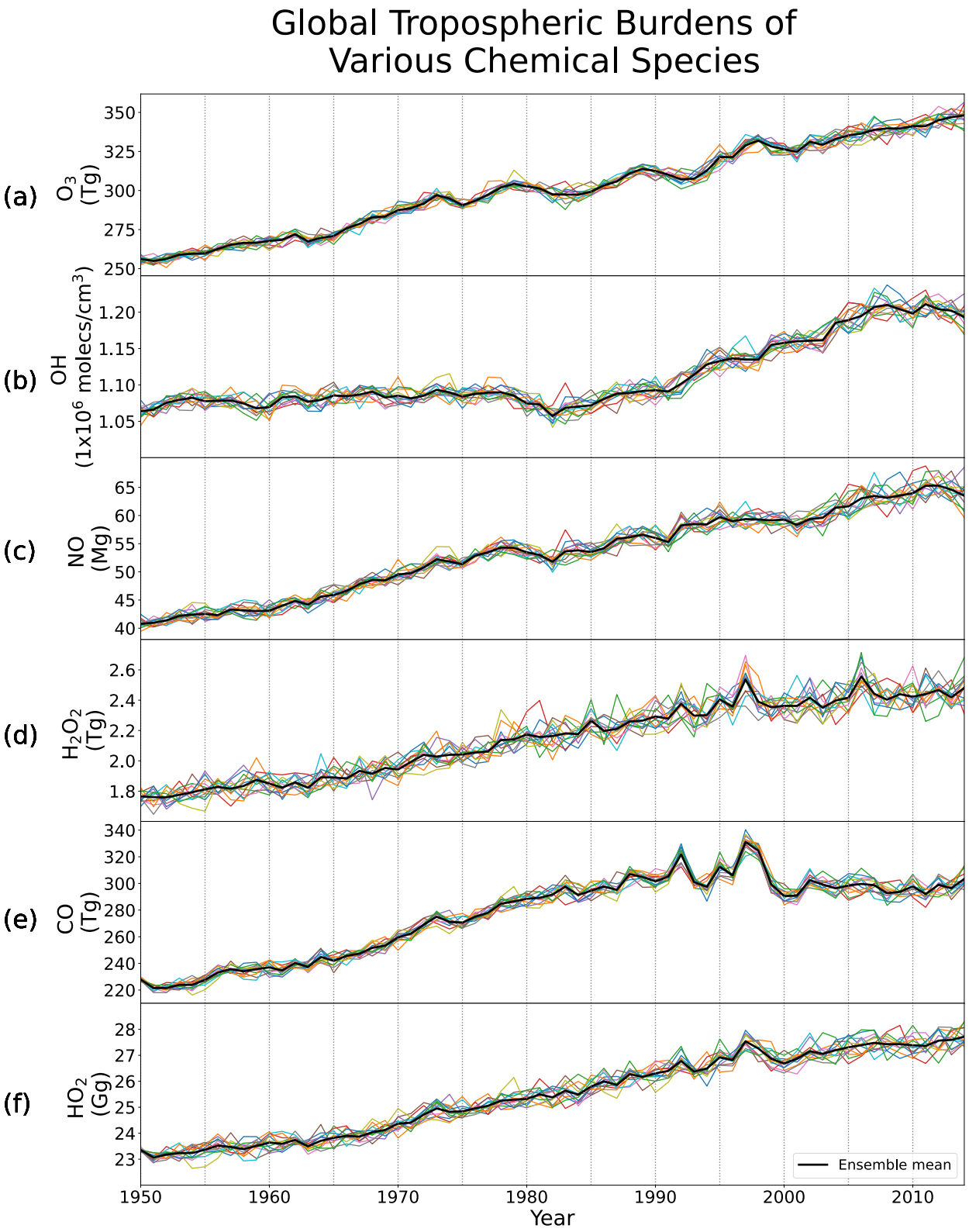

Figure 9: Time series of the global tropospheric (a) O_3 burden, (b) OH Concentration, (c) NO burden, (d) H_2O_2 burden, (e) CO burden, and (f) HO_2 burden. Each colorful line represents a unique ensemble member, with the black line representing the mean across all 13 ensembles.

The fourth subplot in Figure 9 is focused on the H_2O_2 burden. There is a small increase in H_2O_2 prior to 1970, with a relative change of 4.5% over the 1960's, with respect to the annual 1950's burden. This grows to 9.2% in the 1970's, the greatest decade of H_2O_2 increase overall. With more sharp increases and decreases in the 1980's and 1990's, the relative change remains high at 8.7% and 8.6% respectively. This slows down to a 3.1% from 2000 to 2010. We also note large spikes of H_2O_2 burden that are not reflected with sharp increases in OH and O_3. These occur in the years 1992, 1997, and 2006. Anomalies in 1992 and 1997 are associated with increased CO emissions due to biomass burning. The increase in CO causes OH to react to create more HO_2, which self reacts to form H_2O_2. We observe the increases in the CO and HO_2 burdens in Figure 9e and f. This is not the case for the spike in H_2O_2 burden in 2006, as it does not feature the same increases in CO and HO_2 as in 1992 and 1997. We have not ascertained the reason for the 2006 spike, but there may be other chemical or physical mechanisms that are affecting the H_2O_2, which would require further study to understand.

Decade	Absolute Change for each decade, with respect to 1950's			Relative Change for each decade, with respect to 1950's		
	O_3 (Tg)	OH (molecs/cm^3)	H_2O_2 (Gg)	O_3	OH	H_2O_2
1960's	13.1	1.0×10^4	80	5.0%	0.74%	4.45%
1970's	34.3	1.7×10^4	250	13%	1.2%	14%
1980's	42.5	2.8×10^4	400	16%	0.2%	22%
1990's	57.7	6.2×10^4	560	22%	4.5%	31%
2000's	72.9	1.4×10^5	610	28%	10%	34%

Table 3: Change in oxidants per decade, compared to 1950 to 1959 annual burdens of 260.4 Tg (O_3 burden), 1.4×10^6 molecs/cm^3 (OH concentration), and 1800 Gg (H_2O_2 burden).

To better understand the relationships between these various chemical species, we can use scatterplots to determine the strength of the relationship between their ensemble mean burdens. We expect a positive relationship between precursors and products. First, we analyze the relationship between OH burden with H_2O_2 and O_3 in Figures 10 and 11. In both cases, we find that the relationships between these oxidants change abruptly from the time before 1980 and from 1980 forward. For OH and H_2O_2 in Figure 10, we apply an ordinary least squares regression analysis shown by the black line, and note a weak correlation between H_2O_2 and OH, with a coefficient of determination (R^2) value of 0.48 for the pre-1980 time period. The R^2 value rises to a much stronger 0.74 from 1980 forward. This change indicates that the increases in H_2O_2 burden are more closely correlated with changes in OH after 1980. For O_3 and OH shown in Figure 11, we observe an R^2 value of 0.58 before 1980 and 0.93 from 1980 forward. Similar to H_2O_2, ozone is more closely correlated with the

changes in OH from 1980 forward. The change in the coefficient of determination reflects a significant change in OH, which has a small increase from the pre-1980 time period, but has a wider spread and increases rapidly from 1980 forward. The noted shift in relationship between OH and other species in 1980 is also present when comparing its relationship to NO in Figure 12. We generally expect NO to influence OH burden, as NO reacts with HO_2 to form OH in the troposphere (expressed in Reaction 4). This does not happen early on, prior to 1980, with the OH showing little growth, while NO increases substantially. The shift in 1980, similar to the O_3 and H_2O_2 plots, features a sharp increase in the OH from 1980 forward. The R^2 value between NO and OH increases as a result of this regime shift, from a moderate correlation with $R^2 = 0.62$ prior to 1980 and a strong correlation with $R^2 = 0.94$ after 1980.

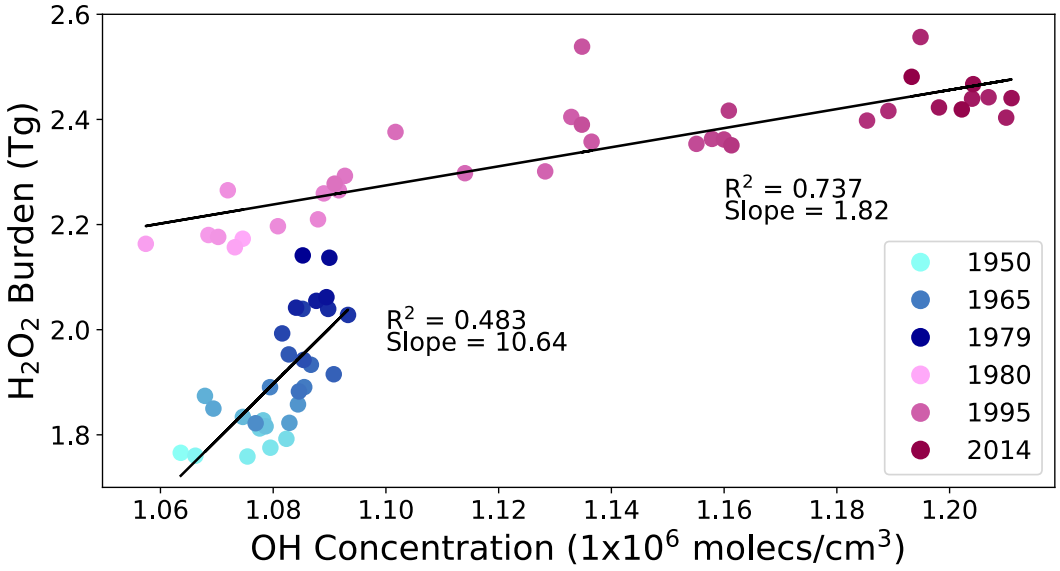

Figure 10: Comparing global annual average tropospheric [OH] and H_2O_2 burden for every year from 1950 to 2014, with each point representing the ensemble mean burden for a single year. Blue points indicate the burdens for 1950 to 1979, with lighter blue representing the earlier years and darker blue representing the later years. Pink points indicate burdens for 1980 to 2014, with lighter pink representing the earlier years and darker pink representing the later years. Black lines show the ordinary least squares regression model, fitted to represent the correlation between the variables.

When comparing ozone burdens with H_2O_2 burdens for our full time period in Figure 13, we see a consistency between their relationship, not interrupted by the shift in OH burden. These oxidants exhibit a strong and nearly linear relationship between O_3 burden and H_2O_2 burden. The R^2 value for the H_2O_2 and O_3 burdens is 0.946 throughout the entire time period, indicating a continuous correlation between global tropospheric O_3 burden and H_2O_2 burden. This suggests that the changes in ozone burden largely influence the changes in H_2O_2 across 1950 to 2014, which contrasts the much smaller role that the changes in OH play in modulating H_2O_2, as shown in Figure 10. It is also clear that although the changes in O_3 over Antarctica play a lesser role in changes in H_2O_2 burden, the changes in

OH concentration drive more of the H_2O_2 burden changes in that area.

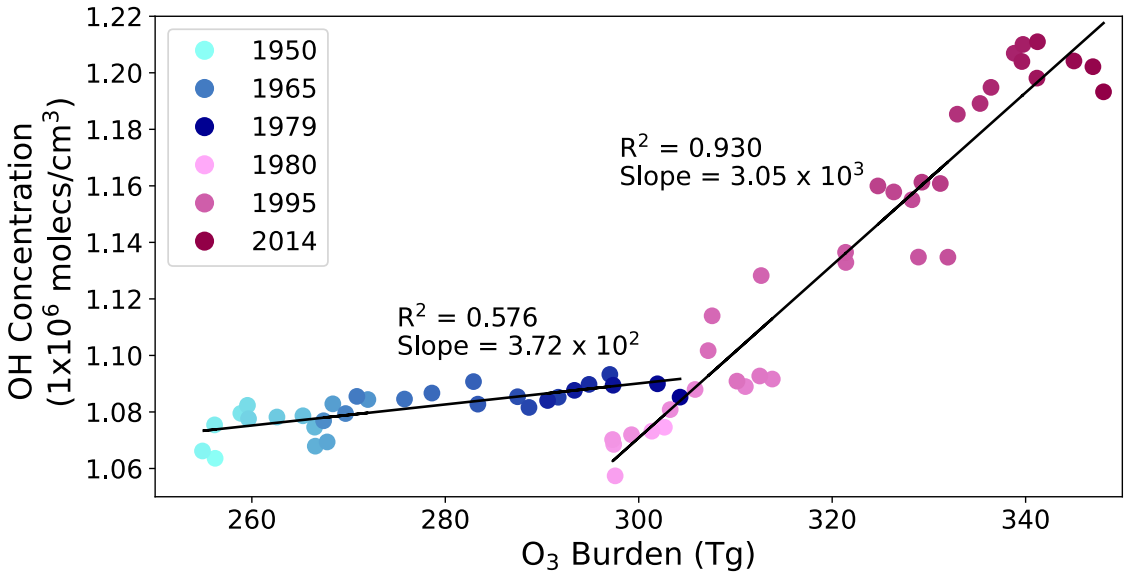

Figure 11: Comparing the relationship between the annual global tropospheric burden for O_3 and [OH]. Each point represents the ensemble mean for the two variables for every year from 1950 to 2014. The blue points indicate the burdens for 1950 to 1979, with the lighter blue representing the earlier years and darker blue representing the later years. The pink indicate the burdens for 1980 to 2014, with the lighter pink representing the earlier years and darker pink representing the later years. Black lines show the ordinary least squares regression model, fitted to represent the correlation between the variables.

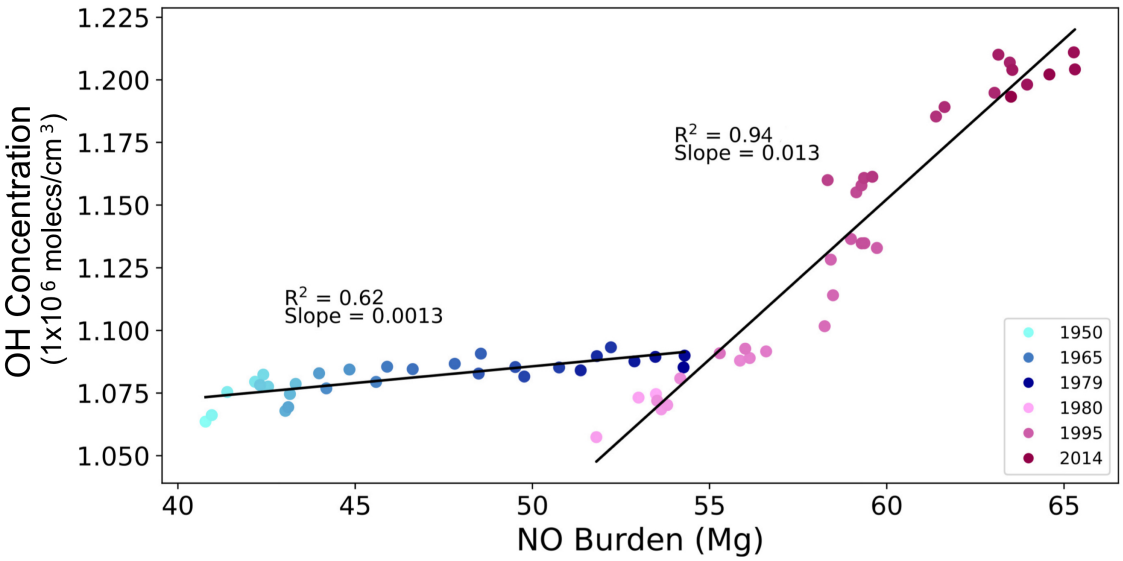

Figure 12: Comparing the relationship between the annual global tropospheric burdens for NO and OH. Each point represents the ensemble mean burden for the two variables for every year from 1950 to 2014. The blue points indicate the burdens for 1950 to 1979, with the lighter blue representing the earlier years and darker blue representing the later years. The pink indicate the burdens for 1980 to 2014, with the lighter pink representing the earlier years and darker pink representing the later years. Black lines show the ordinary least squares regression model, fitted to represent the correlation between the variables.

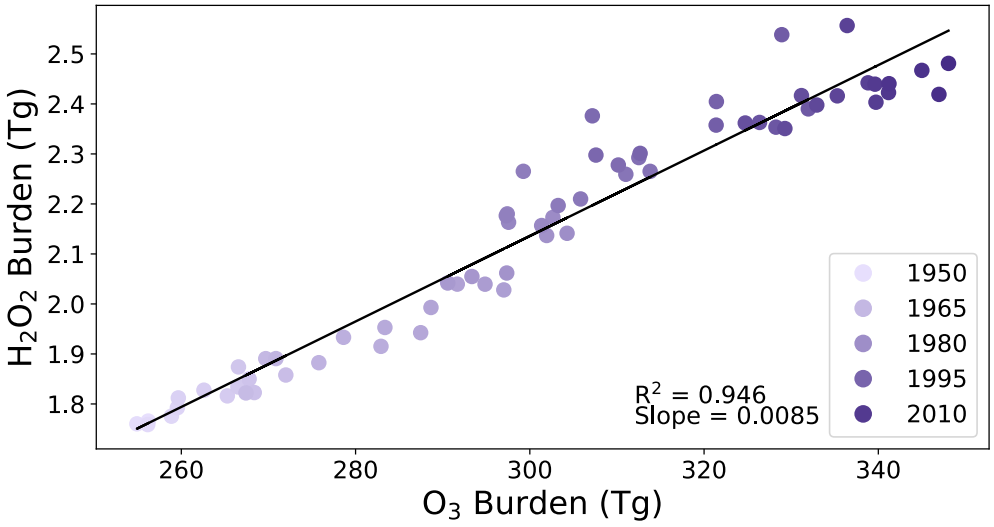

Figure 13: Comparing the global annual tropospheric H_2O_2 and O_3 burdens, each point representing the ensemble mean. The black line shows the ordinary least squares regression model, fitted to represent the correlation between the variables.

4.4 Drivers of Global H_2O_2 Change: Comparing the Dependency of H_2O_2 on $j_{O(^1D)}$ and $j_{O(^1D)}\times$ O_3

In the previous section, we established that the global ozone burden showed a strong correlation with H_2O_2 over our time period, indicating ozone's role as a significant driver of H_2O_2 change from 1950 to 2014. Over Antarctica, changes in OH seemed to be better correlated with changes in H_2O_2. Our main goal in this section is to introduce the photolysis rate coefficient of ozone, $j_{O(^1D)}$, as an additional mechanism that could contribute to the H_2O_2 increase. We also find an overall stronger potential proxy for global H_2O_2 change, the product of both ozone and its photolysis rate, and analyze the relationship between the photolysis rate of ozone and H_2O_2. Lastly, we demonstrate how the combination of O_3 and $j_{O(^1D)}$ is an improved driver of tropospheric H_2O_2 burden over our time period.

With the formation of H_2O_2 primarily described by the process from the initial reaction of O_3 to form HO_x radicals and eventually H_2O_2, we see the photolysis rate of ozone as an important mechanism that contributes to H_2O_2 formation. Reaction 1 portrays the reaction that leads to the dissociation of ozone. In the troposphere, it is roughly independent of altitude but varies greatly by solar zenith angle and therefore latitude (Seinfeld and Pandis 2016). We show the spatial distribution of the mean annual $j_{O(^1D)}$ for 1950 to 1959 from our model output in Figure 14. As the regions near the equator experience longer daylight hours and the solar zenith angle stays at lower angles than at the higher latitudes, the photolysis rate coefficient is generally highest in near the equator and lowest at the poles.

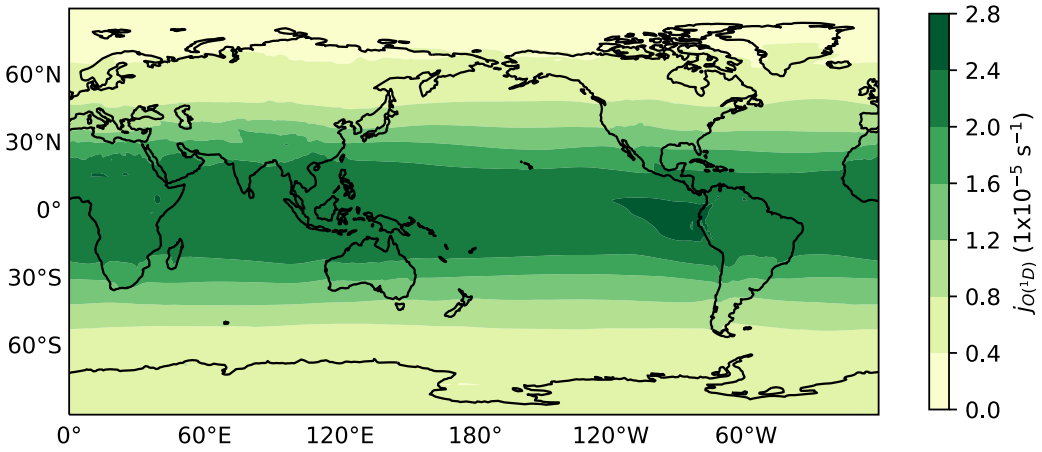

Figure 14: Spatial distribution of annual tropospheric column-averaged photolysis rate coefficient for 1950 to 1959.

As in the previous section, we can examine a scatterplot to analyze the relationship between the annual mean $j_{O(^1D)}$ and H_2O_2 burden, shown in Figure 15. They exhibit a positive relationship and a large spread both in the earlier years and the later years. The R^2 value of 0.72 shows a moderate correlation between the ozone photolysis rate coefficient and the H_2O_2 burden. Changes in $j_{O(^1D)}$ may drive some changes in H_2O_2 burden, but it is not as strong in influencing the global H_2O_2 burden as changes in O_3 burden.

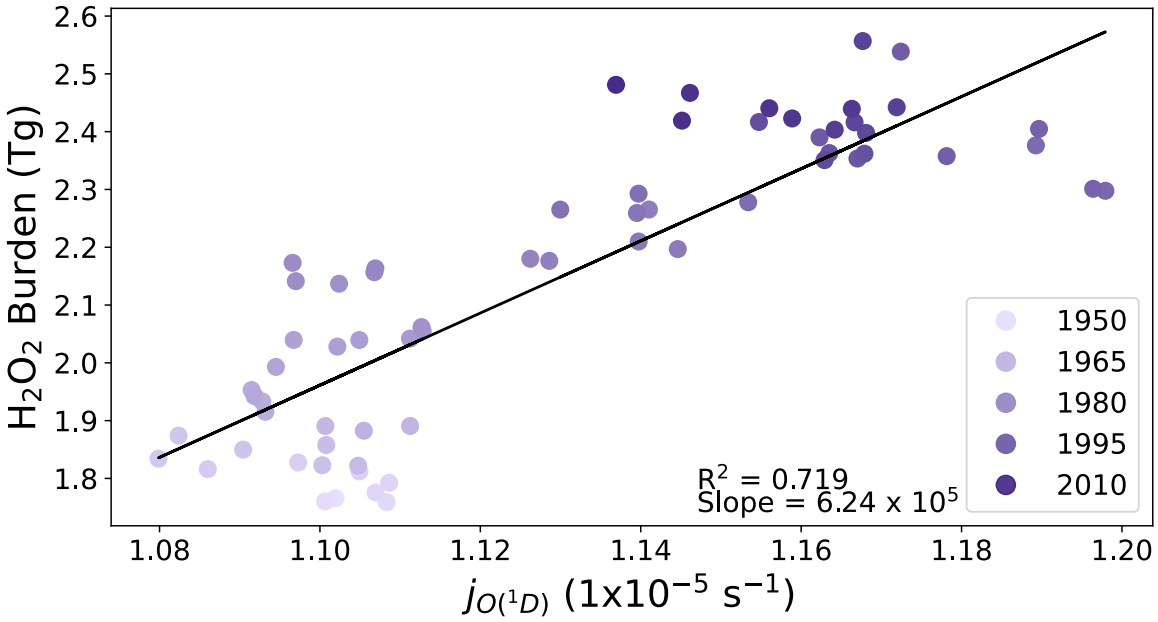

Figure 15: Comparing the global annual mean ozone photolysis rate coefficient with the H_2O_2 burden. Each point represents an ensemble mean value for one year, from 1950 to 2014. Lighter purple points represent the earlier years and darker purple points represent the later years.

A suggested improvement on our previous two potential drivers for H_2O_2 burden change is the product of $j_{O(^1D)}$ and O_3, from Lamarque, McConnell, et al. (2011). They express that areas of low NO_x and alkyl peroxy radicals (RO_2) concentrations, such as in Antarctica, can yield a proportional relationship of HO_2 to the square root of the rate of ozone photolysis and ozone concentrations, as in:

$$[HO_2] \propto \sqrt{j_{O(^1D)} \times [O_3]}.$$

With the formation of H_2O_2 from HO_2 self-reaction and assuming steady state, this becomes:

$$[H_2O_2] \propto j_{O(^1D)} \times [O_3].$$

To evaluate if our global model data aligns with this proportionality, we analyze the association between the global tropospheric H_2O_2 burden and the product of the global annual photolysis rate with the tropospheric O_3 burden in Figure 16. With a higher coefficient of determination ($R^2 = 0.949$) than the plots evaluating the relationship between H_2O_2 burden versus the ozone burden ($R^2 = 0.946$) and $j_{O(^1D)}$ ($R^2 = 0.72$), a combined product of $j_{O(^1D)}$ $\times$ O_3 yields a stronger correlation with H_2O_2 than their separate contributions. Globally, we have seen that H_2O_2 is mostly dependent on ozone, but $j_{O(^1D)} \times$ O_3 is an excellent proxy for H_2O_2 burden overall.

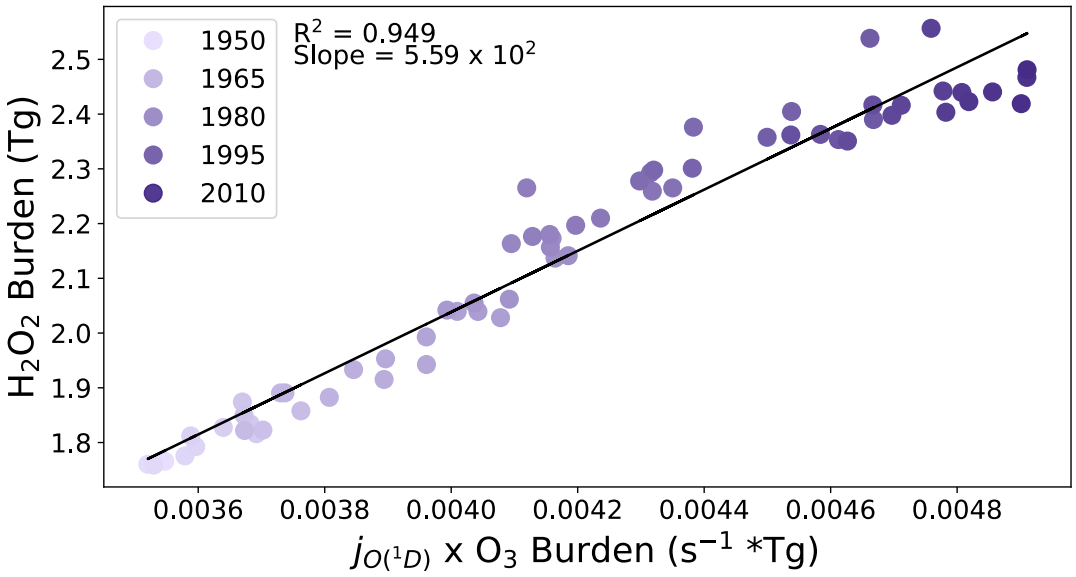

Figure 16: Comparing the global annual mean of the product of the ozone photolysis rate coefficient and the O_3 burden, with the H_2O_2 burden. Each point represents an ensemble mean value for one year, from 1950 to 2014. Lighter purple points represent the earlier years and darker purple points represent the later years.

Now that we have compared the relationship between global H_2O_2 burden with O_3, $j_{O(^1D)}$, OH, and $j_{O(^1D)}\times O_3$ through scatterplots, we can analyze the spatial distribution of the coefficient of determination (R^2). This will improve our understanding of how changes in the ozone burden are a stronger driver of H_2O_2 burden change globally than $j_{O(^1D)}$ and OH, and how this may not be the case in every region. We will also see where $j_{O(^1D)}\times O_3$ is a stronger driver of H_2O_2 change than O_3.

Figure 17a shows the coefficient of determination (R^2) between O_3 and H_2O_2 for 1950 to 2014. We can see the burdens are most highly correlated between 0°and 30°N and S, and more mixed between high and moderate R^2 values below 30°S. Figure 17b shows a lower correlation coefficient between $j_{O(^1D)}$ and H_2O_2 globally, with the highest R^2 values below 45°S. We see that none of the areas in this figure feature as high of a coefficient of determination as in the ozone case. In Figure 17c, we can compare the R^2 value between the OH concentration and H_2O_2. It shows lower R^2 values globally, and notably does not show the same high R^2 as the O_3 and $j_{O(^1D)}$ cases, in much of the region from 15°S to 45°S. There are high R^2 values between H_2O_2 and OH, below 45°S. In line with our conclusions from the initial scatterplots for comparing H_2O_2 with O_3, OH, and $j_{O(^1D)}$, we expect that changes in ozone are driving much of the global H_2O_2 changes from 1950 to 2014 globally. Figure 17d depicts the spatial distribution of the R^2 value between $j_{O(^1D)}\times O_3$ and H_2O_2. This variable ($j_{O(^1D)}\times O_3$) shows a global improvement in the coefficient of determination over the previous variables. The areas of high values between 0°and 30°N and S match the O_3 case, while also improving the coefficient of determination over 60°S to 90 °S. There is also a higher R^2 value in Greenland, which is not as high in the other variables. This comparison to the other variables confirms that the $j_{O(^1D)}\times O_3$ is an improved driver of the changes in H_2O_2 , over the individual O_3, $j_{O(^1D)}$, and OH. It is apparent by looking at all the graphs in

Figure 17 that the mechanism driving most of the H_2O_2 change above approximately 30°S is O_3, while $j_{O(^1D)}$ impacts the changes in H_2O_2 below 30°S.

4.5 Antarctic Case Study: Analyzing the Relationships between Surface H_2O_2 with O_3, $j_{O(^1D)}$, and $j_{O(^1D)} \times O_3$

My analysis for the rest of this thesis focuses on the Southern Hemisphere, particularly Antarctica, to study the changes in one specific region more deeply. Future research can explore the changes occurring in the Northern Hemisphere, and I note more concrete directions for further analysis on that in Section 5.2.2. The emphasis on Antarctica stems from the focus in the literature on the region, due to the availability of ice cores for tracking long-term change for our oxidants of interest. Following some results from Lamarque, McConnell, et al. 2011, we observe our modeled oxidants at the surface level in Antarctica. Then, we evaluate if the relationships between global tropospheric H_2O_2, O_3, $j_{O(^1D)}$, and $j_{O(^1D)} \times O_3$ that were defined earlier in this thesis hold true at the surface level in Antarctica.

I chose the location for this case study based on several observational studies in the literature. Recent cores drilled for H_2O_2 concentrations (Frey, Stewart, et al. 2005; Frey, Bales, and McConnell 2006) and accumulation studies (Banta et al. 2008) were collected largely near the West Antarctic Ice Sheet, at around 79°S, 112°W. Significant findings in Frey, Bales, and McConnell (2006) suggest some optimal conditions for future ice cores taken to study H_2O_2: the most optimal areas to drill when prioritizing H_2O_2 studies are in high-accumulation and low temperature sites. This is because of H_2O_2 can often evaporate quickly after being deposited or be destroyed by photolysis or face decomposition in ice due to dust (Alexander and Mickley 2015). These processes may compromise accurate interpretations from ice core records, thus future sampling should be carefully planned to avoid as many of these issues as possible. One example in which these post-depositional processes may have caused significant issues were in Siple Station Antarctic ice cores from Sigg and Neftel (1991), which showed no obvious trend in H_2O_2 between 1900 and 1980 (Thompson 1992). The cores around 79°S, 112°W appeared to be in an area of high-accumulation and low temperature, prompting my usage of the closest location in our model data, around 79.6°S, 112.5°W.

Before beginning our analysis, we can speculate on the trends we should expect to see, given some background from the literature. Frey, Bales, and McConnell (2006) identified an increase in H_2O_2 after 1950 in all their ice cores, with over 20 analyzed in their study. Lamarque, McConnell, et al. 2011 narrowed the window down to post-1970. H_2O_2 increases are attributed to the changes in tropospheric ozone and stratospheric ozone in Frey, Stewart, et al. (2005) and Lamarque, McConnell, et al. (2011), but these studies identify that in Antarctica, the changes in stratospheric ozone are the main drivers in H_2O_2 increase, through their effects on the ozone photolysis rate. These stratospheric ozone changes involve the significant springtime depletion of stratospheric ozone above Antarctica, post 1980, due to the formation of polar stratospheric clouds that promote heterogeneous reactions leading to ozone loss (Seinfeld and Pandis 2016). The stratospheric O_3 depletion increases UV-B radiation into the troposphere, which promotes the photolysis of ozone by Reaction 1 and thus stimulates $j_{O(^1D)}$, formation of OH, and H_2O_2 (Frey, Stewart, et al. 2005; Anklin and Bales 1997; Schnell, Liu, et al. 1991; Fuglestved, Jonson, and Isaksen 1994). This would also

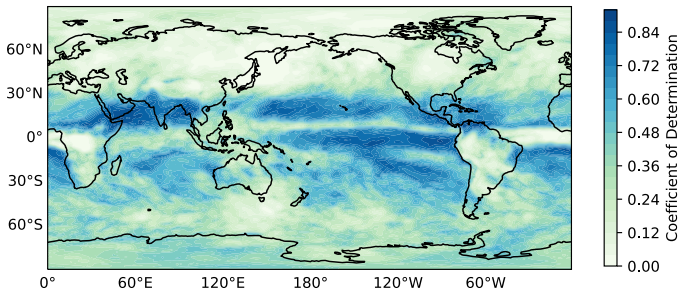

(a) O_3

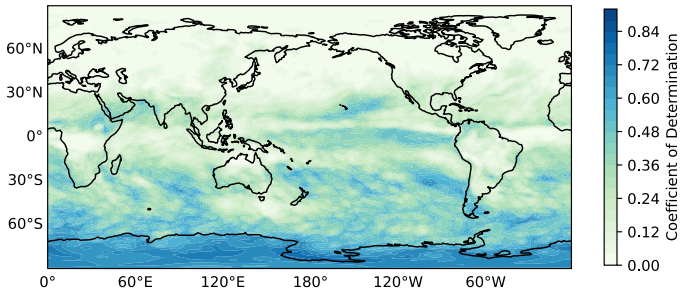

(b) $j_{O(^1D)}$

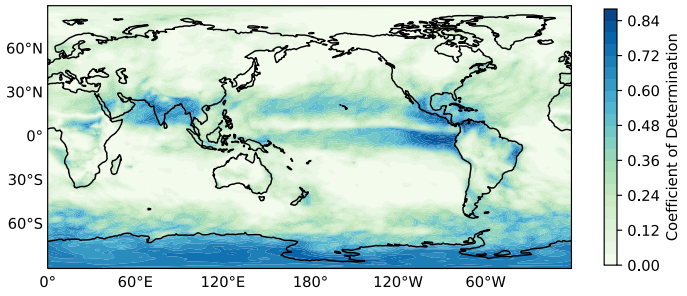

(c) OH

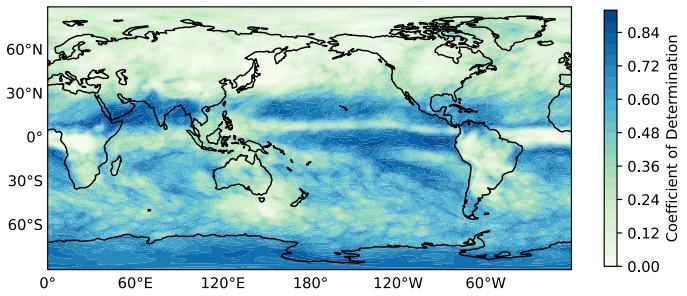

(d) $j_{O(^1D)} \times O_3$

Figure 17: Spatial distribution of the coefficient of determination between ensemble mean, annual mean tropospheric H_2O_2 burden with (a) annual mean tropospheric O_3 burden, (b) column-averaged annual mean tropospheric $j_{O(^1D)}$, (c) annual mean tropospheric OH concentration, and (d) annual mean $j_{O(^1D)} \times O_3$ burden, from 1950 to 2014.

result in a decrease in tropospheric ozone in Antarctica, as more of the ozone is undergoing photolysis. Then, in looking at the changes in O_3 burden, $j_{O(^1D)}$, OH concentration, and H_2O_2 burden, we should expect decreases in ozone, increases in $j_{O(^1D)}$, increases in OH, and increases in H_2O_2. If more of the changes in H_2O_2 are driven by changes in stratospheric ozone and therefore $j_{O(^1D)}$, we can also expect to see a stronger correlation between $j_{O(^1D)}$ and H_2O_2 in Antarctica than O_3 and H_2O_2. With low levels of NO_x, we can predict improved agreement from the product of $j_{O(^1D)}\times$ O_3, in comparison to solely O_3 or $j_{O(^1D)}$. These expectations are all concentrated on changes in the overall troposphere, which may not be the case at the surface level. Thus, we set out to see if our data match our assumptions.

Our model's surface volume mixing ratios for H_2O_2 and O_3 at the approximate ice core for 1950 to 2014 is shown in Figure 18. The declines in surface ozone in Figure 18a, from the 1980's and 1990's, show the effects of stratospheric ozone depletion during the time period (with an increase in $j_{O(^1D)}$ serving as a sink for ozone). In our Figure 18b time series, we can see spikes in H_2O_2, most apparent in 1980, 1995, and through the 1990's. The increases we observe support the findings of the Lamarque, McConnell, et al. (2011) study using the CAM-chem and G-PUCCINI models identifying an increase in H_2O_2 starting in the 1970's.

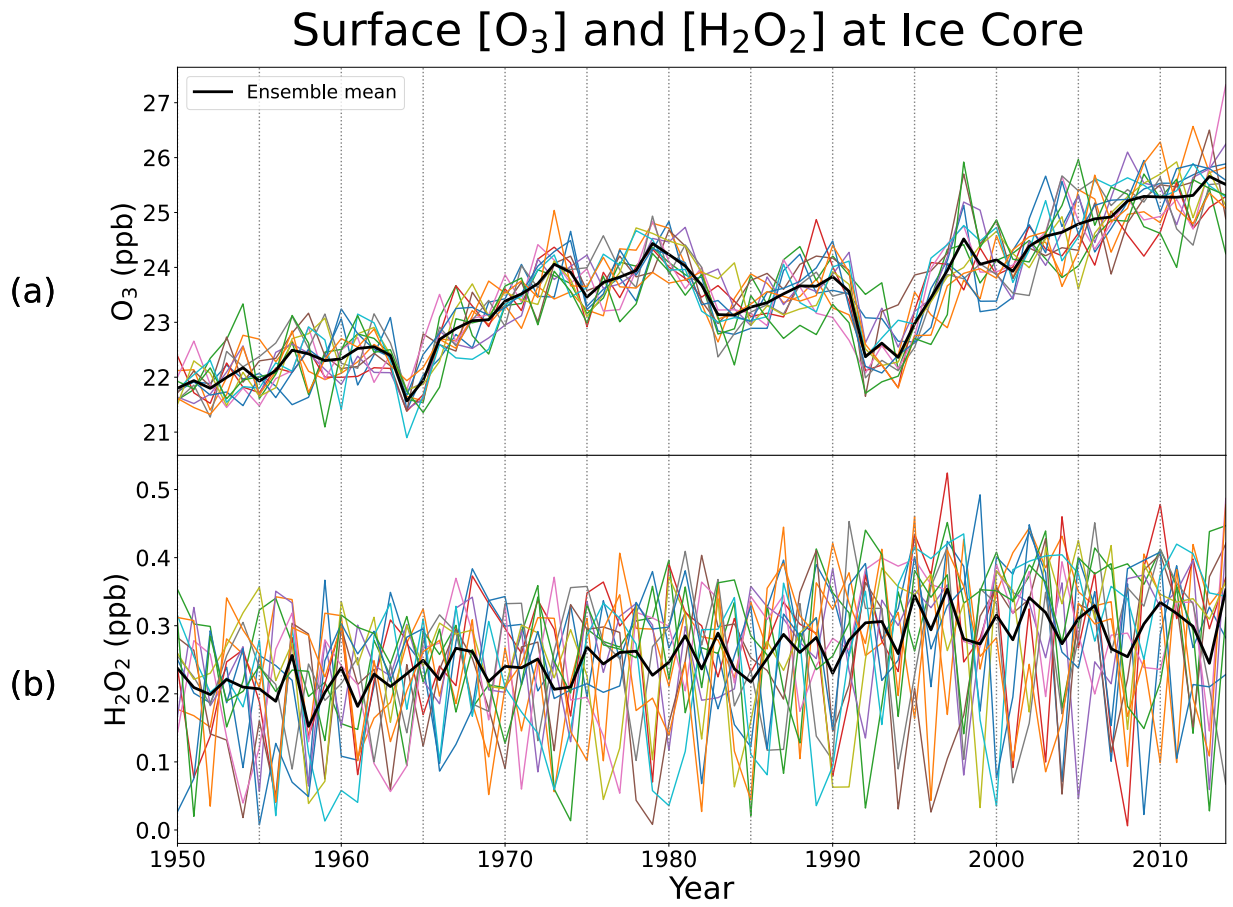

Figure 18: Surface H_2O_2 and O_3 concentrations at the ice core location from 1950 to 2014. The colored lines denote each ensemble member, with the solid black line representing the ensemble mean.

Figure 19 depicts the same time series plot as Figure 18b, but includes volume mixing ratios of surface and near-surface gas-phase observations taken in the 1980's to early 2000's from Jacob and Klockow (1993), Fuhrer, Hutterli, and McConnell (1996), McConnell et al. (1997), Riedel et al. (2000), Hutterli, McConnell, Chen, et al. (2004), and Frey, Stewart, et al. (2005). These observations were taken during the summer, when H_2O_2 is at its highest, while our simulations represent annual means. The measurements help us to ensure that our simulations estimate reasonable values for $[H_2O_2]$ in Antarctica. We can see that our model's values fall within the range of the majority of the observations. Note that some of the measurements are maximums, such as those from Fuhrer, Hutterli, and McConnell (1996), denoted by cyan stars in the plot, so although the points are above our estimated H_2O_2, it may be that the mean H_2O_2 from those studies would be in a reasonable range aligning with our simulations. One limitation is that these measurements were taken in different areas of Antarctica, not specifically at the ice core location. Frey, Stewart, et al. (2005) noted that this meant their mean H_2O_2 concentrations for 2000 and 2002, taken in West Antarctica, were 1.6 times the mean of observations taken in Riedel et al. (2000), while the ranges were comparable (30-900 ppt).

Analyzing the relationship between the ensemble mean for $[O_3]$ and $[H_2O_2]$ at the ice core in Figure 20, we see a much larger spread in the data than in the global example. There is a very weak correlation between the two chemical species, with an R^2 value of 0.335. The same analysis is performed for the mean photolysis rate coefficient at the ice core location in Figure 21. We observe a stronger correlation between $j_{O(^1D)}$ and H_2O_2 than in the O_3 and H_2O_2 comparison, with an R^2 value of 0.529.

Similar to the global analysis, we see the best agreement to H_2O_2 with a combination of O_3 and $j_{O(^1D)}$. Figure 22 shows the scatterplot depicting the relationship between $j_{O(^1D)} \times [O_3]$. The $R^2 = 0.585$ value is the highest for our Antarctic case study thus far, suggesting that H_2O_2 is somewhat modulated by both the mechanisms. The $j_{O(^1D)}$ plays the larger role in the individual case, although we observe that the overall R^2 value is moderate, not strong. Therefore, in our surface level study of H_2O_2 changes over Antarctica in this section, we conclude that our findings agree with Frey, Stewart, et al. (2005) and Lamarque, McConnell, et al. (2011) that changes in $j_{O(^1D)}$ contribute to changes in H_2O_2.

One limitation of our case study is that the analysis is focused on one singular grid square in our model output. We can conduct further analysis over a larger Antarctic area, averaging over three ice core locations, which was utilized in Lamarque, McConnell, et al. (2011), or over the entire Antarctic land mass. Averaging over more significant area may provide increased certainty in our data than our current analysis reflects. Despite this issue, we are confident that our H_2O_2 volume mixing ratios at surface level are reasonable, given the comparison to various gas-phase measurements in Figure 19.

4.6 Initial Findings from ODS-Fixed Simulations: Exploring the Potential Role of Stratospheric Ozone Depletion

In comparing the relationships between O_3, $j_{O(^1D)}$, and H_2O_2 in the previous two sections, we discerned some differences between the global and Antarctic trends, with the global study showing a larger dependency for H_2O_2 change on O_3 change and the Antarctic study showing

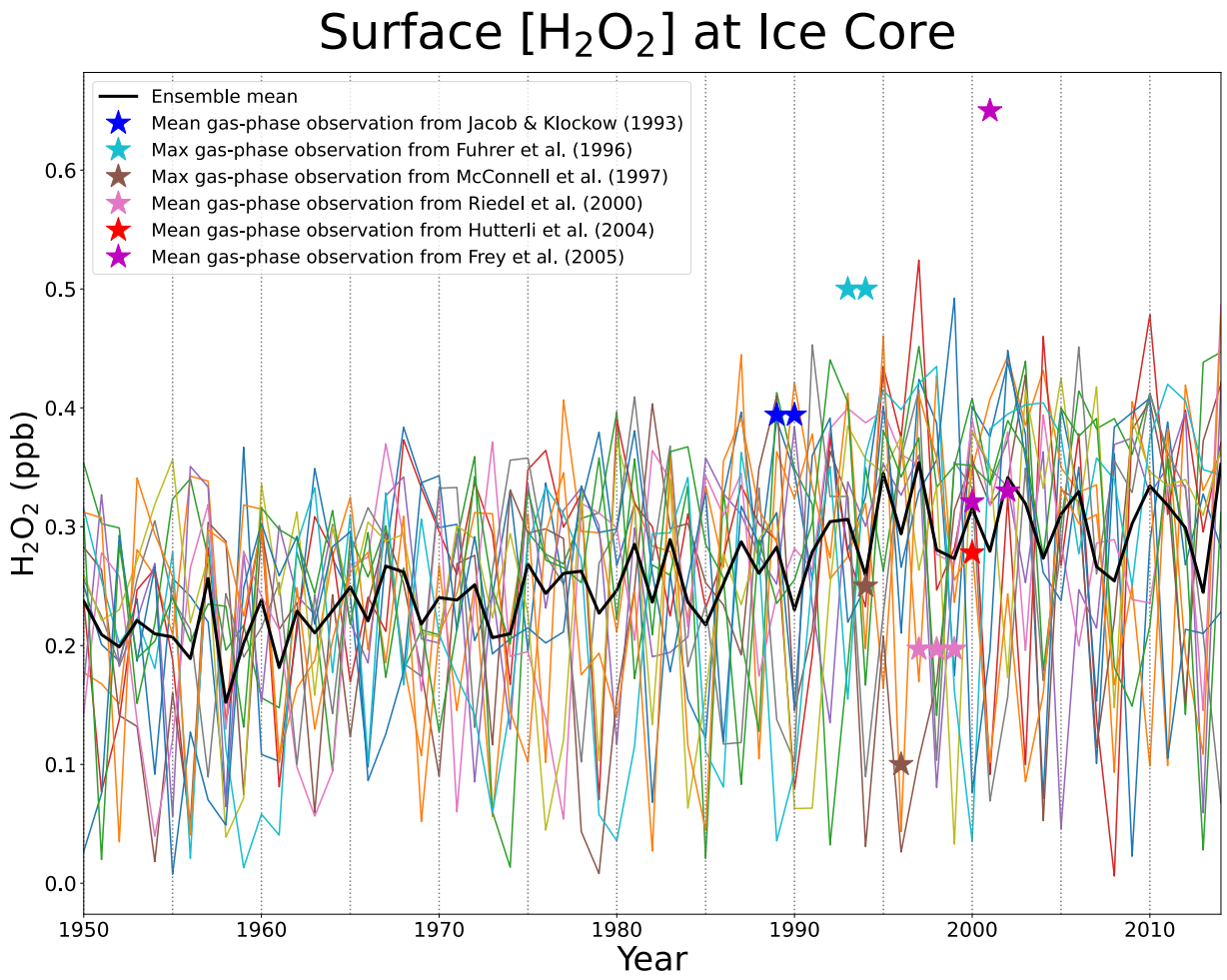

Figure 19: Time series depicts surface H_2O_2 volume mixing ratios for the grid cell nearest to the ice core location, from 1950 to 2014. Colored lines denote individual ensemble members, with the solid black line denoting the ensemble mean. Stars indicate observations taken in Antarctica through various studies in the literature, all taken during summer.

a larger dependency for H_2O_2 change on $j_{O(^1D)}$. Both showed improvements in the product of ozone and its photolysis rate. We identified their differences as being potentially connected to stratospheric ozone depletion, which should affect Antarctica considerably greater than most of the world. To test the impact of stratospheric ozone depletion specifically on H_2O_2, we perform our same analysis applied to the original simulations to a set of parallel simulations, which hold ozone depleting substances at 1950 levels. In these simulations, the stratospheric ozone depletion from the 1980's forward does not occur, no longer perturbing tropospheric O_3, $j_{O(^1D)}$, and all other associated changes. There are only four ODS-fixed ensemble members, which are comparable to the first four original simulations and end in 2013. For the rest of this paper, the initial simulations will be referred to as "historical simulations," and the simulations where ozone depletion does not occur will be referred to as the "ODS-fixed simulations." As the ODS-fixed simulations end in 2013, we thus limit our study from 1950 to 2013. We can expect that if stratospheric ozone depletion drove changes in

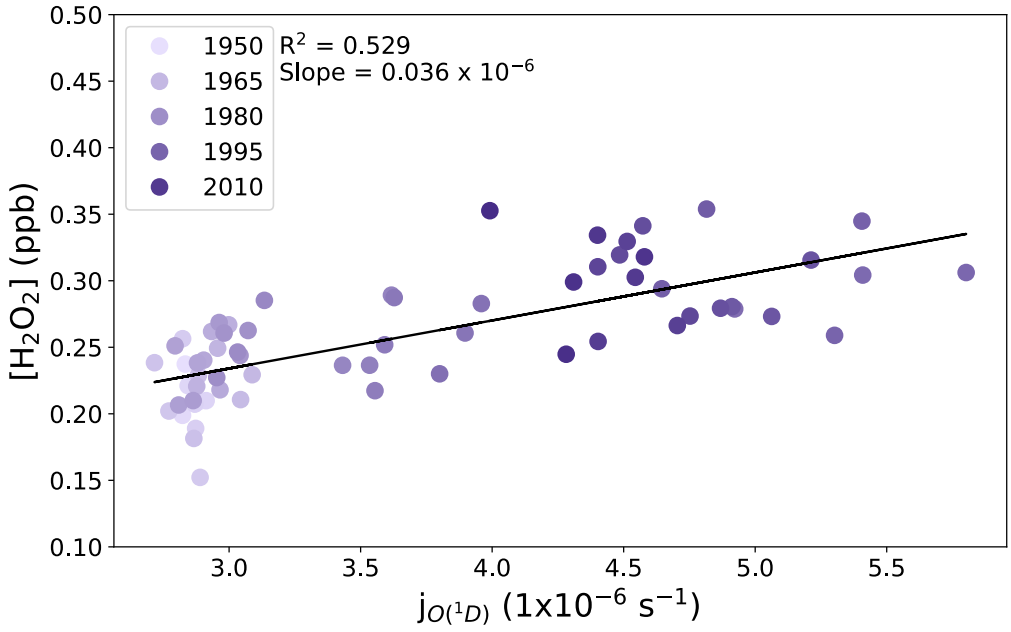

Figure 20: Scatterplot depicting the relationship between surface $j_{O(^1D)}$ and H_2O_2 at the ice core. Each point represents an ensemble mean value for one year, from 1950 to 2014. Lighter purple points represent the earlier years and darker purple points represent the later years. The black line describes the ordinary least squares regression fit for the data.

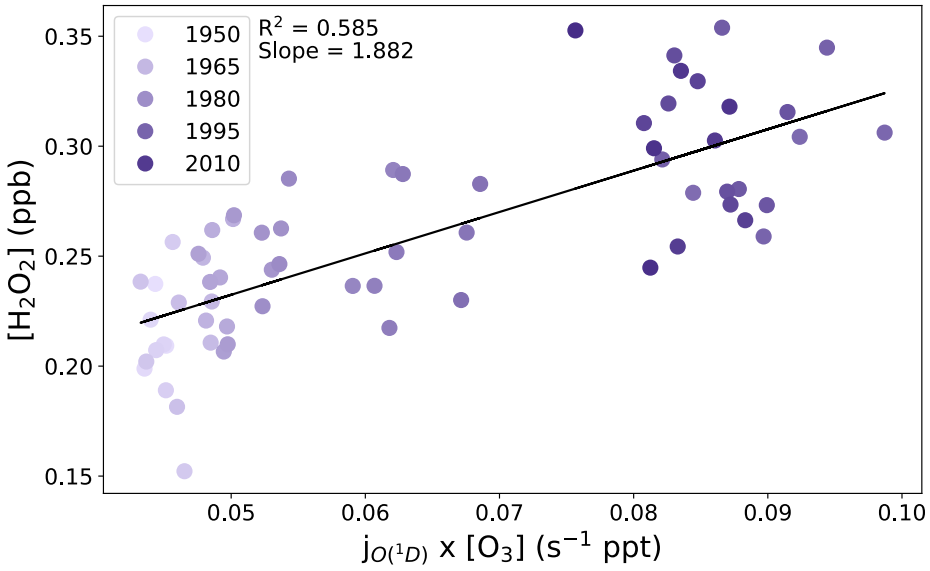

Figure 21: Scatterplot depicting the relationship between the ozone photolysis rate coefficient and hydrogen peroxide at the ice core location. Each point represents an ensemble mean value for one year, from 1950 to 2014. Lighter purple points represent the earlier years and darker purple points represent the later years. The black line describes the ordinary least squares regression fit for the data.

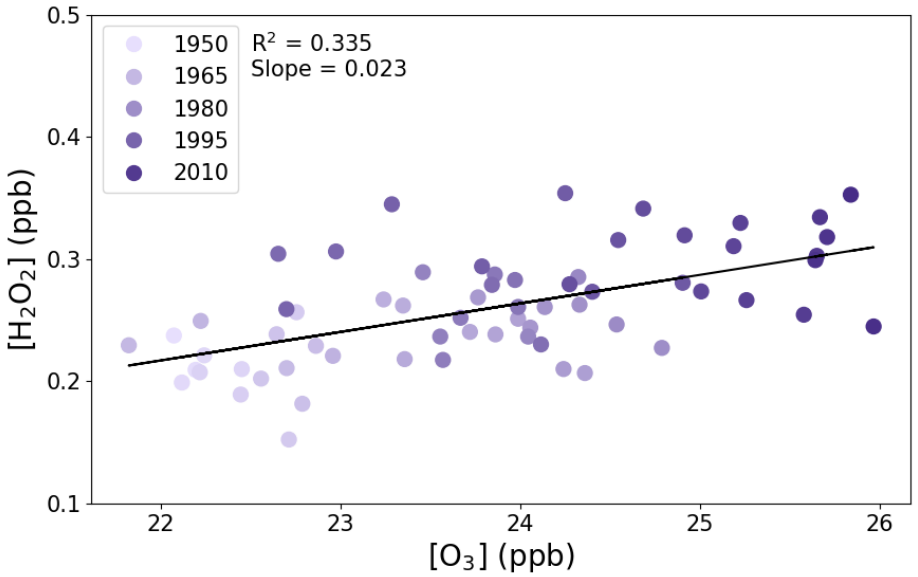

Figure 22: Scatterplot depicting the relationship between $[O_3]$ and $[H_2O_2]$ at the ice core location. Each point represents an ensemble mean value for one year, from 1950 to 2014. Lighter purple points represent the earlier years and darker purple points represent the later years. The black line describes the ordinary least squares regression fit for the data.

H_2O_2 between 1950 and 2013, we will observe significant differences between these ODS-fixed simulations and our historical runs. This is because we identified the effect of stratospheric ozone depletion in increasing $j_{O(^1D)}$ as a potential mechanism for H_2O_2 increases over our time period.

We first compare the H_2O_2 burden in the global data between the historical and ODS-fixed simulations in Figure 23 across our time period. In the time series, the ensemble mean for the four historical simulations is depicted in black, while the ensemble mean burden for the ODS-fixed simulations is in blue. In place of the usual individual ensemble members, there is a gray shaded area depicting the total spread of the H_2O_2 burden, with the upper bound indicating the maximum burden value across the four ensembles and the lower bound as the minimum burden. The blue shaded region similarly defines the maximum and minimum burdens for the ODS-fixed simulations. Our two ensemble means show strong agreement both in general trend and in their spread, with the mean historical simulations staying within the shaded bounds of the ODS-fixed simulations. This indicates that the difference between the H_2O_2 burden for the historical and ODS-fixed simulations is a result of internal climate variability. As the ODS-fixed simulations depict how the H_2O_2 burden would be without the effects of ozone depleting substances, our plot indicates that the effects of stratospheric ozone depletion (particularly impactful in the 1980's and 1990's) does not have an overall meaningful impact on the global annual average hydrogen peroxide burden. If the increase in H_2O_2 was driven by the stratospheric ozone depletion, yielding a higher $j_{O(^1D)}$ and more conversion of ozone to eventually form H_2O_2, we would expect to see a significantly higher H_2O_2 burden in the historical simulations than the ODS-fixed values.

For the global tropospheric ozone burden in Figure 24, we find generally close agreement

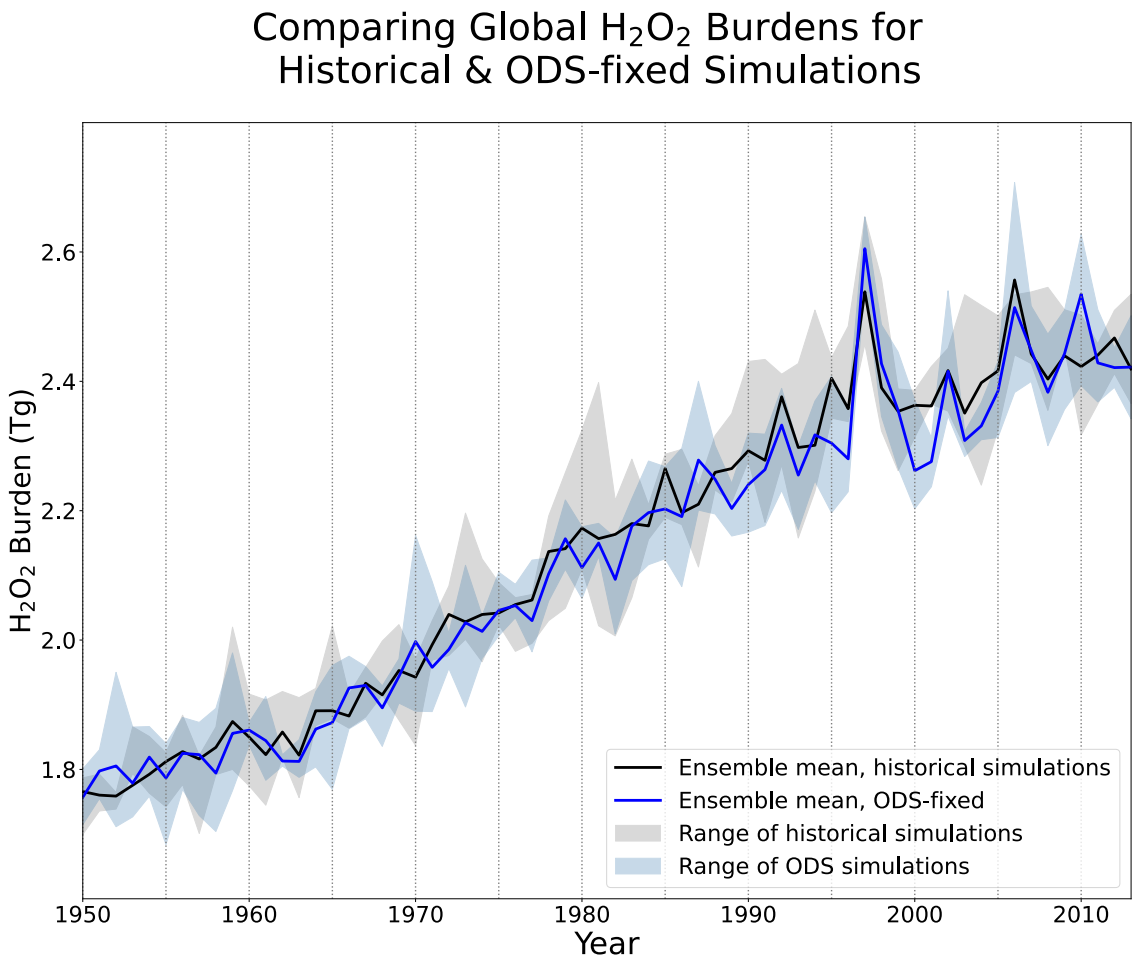

Figure 23: Global tropospheric H_2O_2 burdens from 1950 to 2013. The ensemble mean for the original 13 ensembles is depicted in black, while the ensemble mean burden for the parallel simulations is in blue. The gray shaded area represents the maximum and minimum H_2O_2 burden across the ensemble spread for the original 13 members.

in trend and spread between the original and parallel simulations in the earlier years. Trends in the ensemble member means for the two sets of simulations remain roughly similar through the entire time period. What stands out is the divergence in the spread starting in the 1970's. The difference between the simulated values becomes more pronounced in the 1980's, as the ensemble mean for the historical simulations drops below the shaded ODS-fixed area, demonstrating the response to an external forcing (stratospheric ozone depletion). Thus, the stratospheric ozone depletion may have played a role in the decrease of the global annual tropospheric ozone burden worldwide from the 1980's forward.

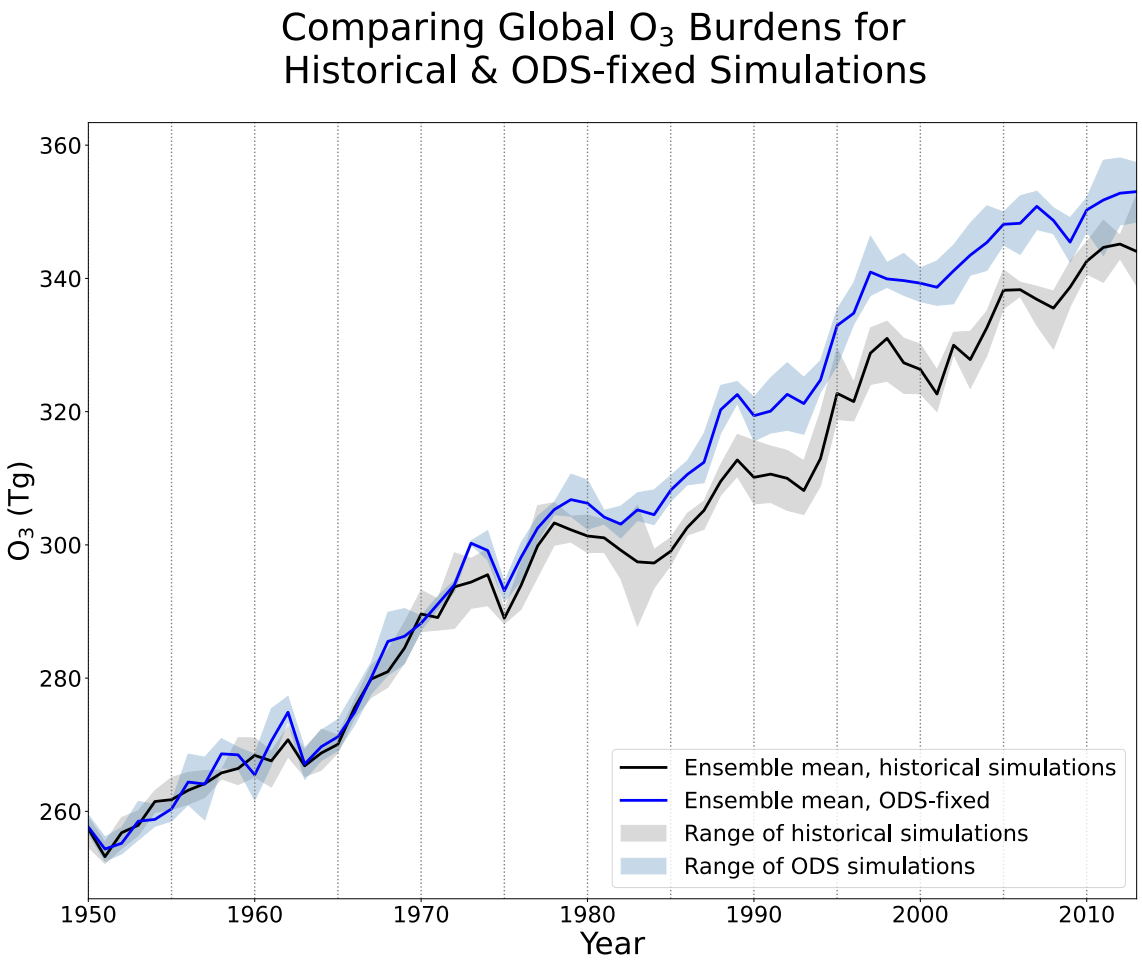

Figure 24: Global tropospheric O_3 burdens from 1950 to 2013. The ensemble mean for the historical ensembles is depicted in black, while the ensemble mean for the ODS-fixed simulations is in blue. Their increasing distance in the 1980's quantifies the effect of stratospheric ozone depletion on the tropospheric burden. The gray shaded region indicates the maximum and minimum O_3 burden across the ensemble spread for the four historical ensemble members, and the blue shaded region indicates the maximum O_3 burden for the ODS-fixed simulations.

Finally, we compare the $j_{O(^1D)} \times O_3$ for the two simulation types in Figure 25. The overall trend roughly follows the shape of the previous ozone burden plot (Figure 24) for both the historical and ODS-fixed simulations, demonstrating the larger influence of O_3 on the product. With the photolysis rate's contributions, the ensemble mean from the historical simulations is generally greater than the ensemble mean of the ODS-fixed simulations. After 1980, there is no large difference between the two sets of simulations, indicating that the product of O_3 and $j_{O(^1D)}$. Thus, the global annual mean $j_{O(^1D)} \times O_3$ burden does not show convincing evidence of impact from stratospheric ozone depletion.

We emphasize that our conclusion of H_2O_2 not being impacted significantly by stratospheric ozone depletion is not unique. Although studies such as Lamarque, McConnell, et al. (2011) and Frey, Stewart, et al. (2005) attributed the increases in H_2O_2 to increases in $j_{O(^1D)}$

and therefore stratospheric ozone depletion, other papers found that periods of stratospheric depletion yielded no differences in H_2O_2. These include Riedel et al. (2000), which found that the H_2O_2 mixing ratios were similar to the typical wintertime values. Anklin and Bales (1997) proposed that changes in tropospheric chemistry had to also play a role for H_2O_2 they observed in Greenland, including changes in NO_x, CO, and methane. Another species that may play a role is water vapor, which has been increasing due to global warming. Anklin and Bales (1997) postulates that increased global warming could increase humidity and fog events, which have been shown to increase H_2O_2 on the surface.

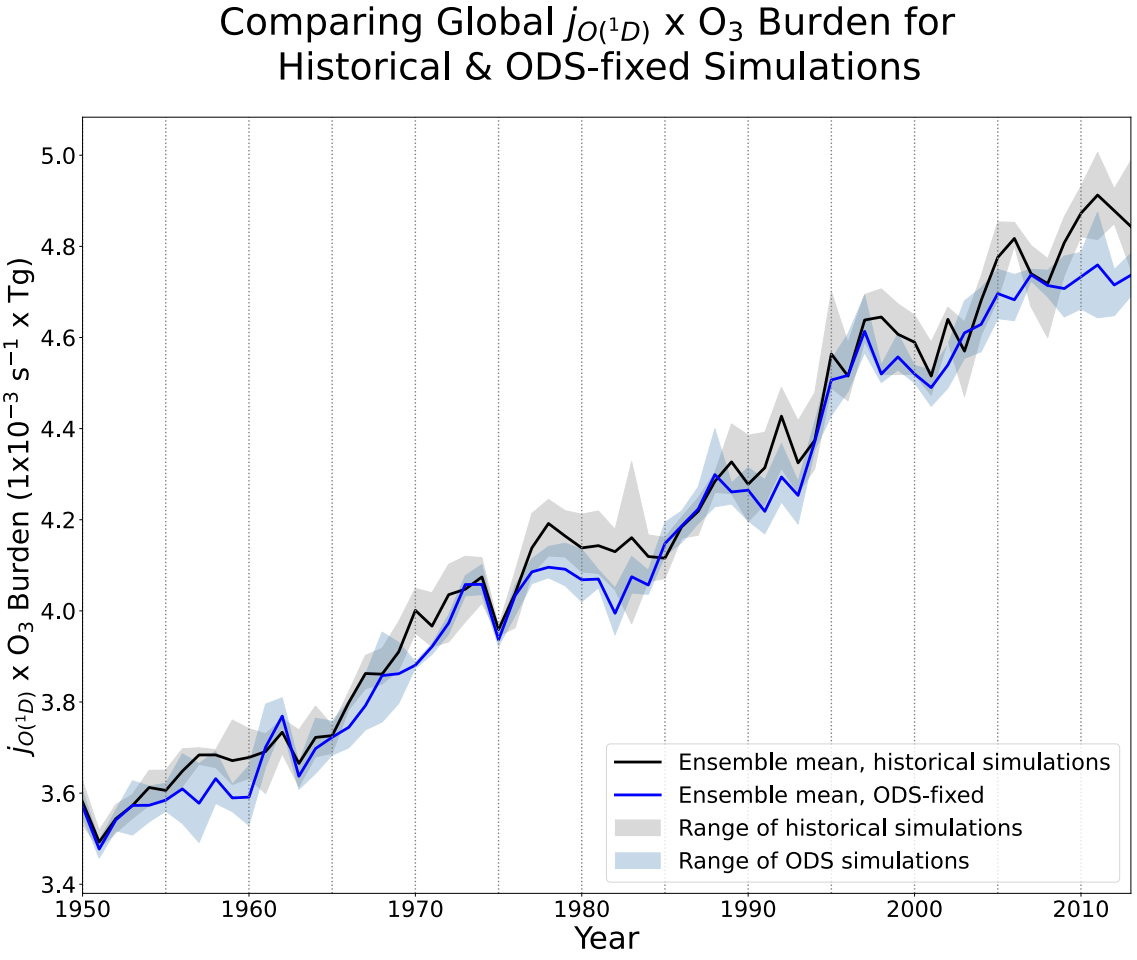

Figure 25: Global $j_{O(^1D)} \times O_3$ burden from 1950 to 2013. The ensemble mean for the historical ensembles is depicted in black, while the ensemble mean for the ODS-fixed simulations is in blue. The gray shaded region indicates the maximum and minimum O_3 burden across the ensemble spread for the four historical ensemble members, and the blue shaded region indicates the maximum O_3 burden for the ODS-fixed simulations.

While there was no discernible impact of stratospheric ozone depletion on the global annual mean H_2O_2 burden in these simulation comparison plots, further analysis may illuminate regional differences where the depletion is a clear forcer for changes in H_2O_2 burden. For example, the same analysis performed over the Antarctic land mass may yield different

results. The result suggests that other mechanisms, potentially chemical or physical, could be responsible for driving H_2O_2 burden change.

5 Conclusions and the Way Ahead

5.1 Summary

In this paper, we improved our understanding of how H_2O_2 is related to various processes that control its trends both globally and over Antarctica. H_2O_2 plays a significant role as a sink of HO_xradicals, making it a key oxidant of study. We quantified the changes in H_2O_2 burden for our time period, finding that the Northern Hemisphere had a greater absolute change but Southern Hemisphere had a greater relative change, as shown in Table 2. We showed the spatial distribution of the deposition rate and estimated approximate lifetimes for H_2O_2 with respect to depositional processes (around 2.8 days for wet and dry deposition combined), to better understand the sinks for H_2O_2 . We compared oxidant burdens to show that the rates of change are not the same across our oxidants. Ozone and H_2O_2 presented improved correlation with OH from 1980 forward, with earlier R^2 values of 0.58 (O_3) and 0.48 (H_2O_2), then improving to 0.9 (O_3) and 0.74 (H_2O_2). From analyzing the changes in ozone photolysis rate coefficient spatial distribution, we theorized that stratospheric ozone depletion may have provided an explanation for more significant relative change in the Southern Hemisphere. We found a moderate correlation between tropospheric O_3 and H_2O_2, but an even stronger correlation for the product of $j_{O(^1D)}$ and O_3 with H_2O_2 at the surface in Antarctica. At our ice core location, we found lower R^2 values than in the global case, but this may be due to averaging over a single grid cell rather than all of Antarctica or several locations. We expected a strong correlation between $j_{O(^1D)}$ and H_2O_2, as the stratospheric O_3 depletion boosts the $j_{O(^1D)}$ rate by stimulating ozone photolysis. The improvement in the coefficient of determination for the combined changes of $j_{O(^1D)} \times O_3$ shows us that changes in both $j_{O(^1D)}$ and O_3 could potentially be driving H_2O_2 burden increases in the 1970's and beyond (as suggested by Lamarque, McConnell, et al. (2011)). Lastly, by comparing our simulations to a parallel set of simulations with ozone depleting substances fixed at 1950 levels, we found that changes in H_2O_2 were likely not severely influenced by stratospheric ozone depletion after all, with the differences in the H_2O_2 burden in the two simulation sets largely due to internal climate variability. Further study is necessary to continue determining why stratospheric ozone may not be the forcing that propels the increases in H_2O_2 .

5.2 Future Work

5.2.1 Comparison with observational data

Field campaigns have yielded more modern H_2O_2 aqueous and gas-phase measurements that can be used to ascertain how well our model matches real-world observations. The airborne flights include several large-scale NASA missions where they measured a large variety of gases and smaller field campaigns that focused on H_2O_2 specifically (Tilmes et al. 2015; Kelly, Daum, and Schwartz 1985; Heikes, Kok, et al. 1987; Heikes, Walega, et al. 1988; Barth et al. 1989; Atlas and Ridley 1996; Ridley et al. 1997; Staffelbach, Kok, et al. 1996;

O'Sullivan et al. 1999; Singh, Thompson, and Schlager 1999; Wang, Ridley, et al. 2003; Olson et al. 2012). In particular, the papers summarizing results of these field campaigns are often used to create vertical profiles of H_2O_2 concentrations at various times and locations. We can create similar vertical profiles with our model outputs and compare them to the experimental results from these campaigns. This will help us to study more local changes and understand the vertical distribution of H_2O_2 between the upper, middle, and lower troposphere, which could help us find additional mechanisms for the H_2O_2 burden increases.

5.2.2 Effect of Sulfur Dioxide Emissions on H_2O_2

One considerable finding that we allude to early in this paper when examining the overall H_2O_2 global distribution and trends is that there is a distinct difference between Northern Hemisphere and Southern Hemisphere H_2O_2 burden changes. This is emphasized by all past modeling studies and ice core studies in the literature, as mentioned in Section 2.2. Moller (1999) postulated that the difference is due to H_2O_2 reactions related to SO_2 emissions that occur in the Northern Hemisphere but do not affect the Southern Hemisphere.

These reactions suggest that a decrease in SO_2, largely due to decreased emissions as a result of the Clean Air Act, should lead to an increase in H_2O_2, as the H_2O_2 is no longer reacting with HSO_3^-. To explore this idea, we can compare the SO_2 burden in our model data to see if there is a correlation with our H_2O_2 burden. We should also see an associated decrease in the final product, sulfuric acid. H_2SO_4 exists as its own H_2SO_4-H_2O droplets (Seinfeld and Pandis 2016), but also serves as an important component for forming sulfate aerosol particles, taking part in reactions to modify particles (Stolzenburg et al. 2020). Therefore, we would also see a reduction in sulfate aerosols with the decrease in SO_2 emissions. If these trends occur together in our model data, it would support the connection between the SO_2 and H_2O_2 in Greenland ice cores. Moller (1999) suggests that the relationship would not exist in the Southern Hemisphere, so further work in this area could highlight a key factor in the differences in H_2O_2 concentrations in Greenland versus Antarctic ice cores and the different trends across the two hemispheres overall.

6 List of Figures

7 List of Tables

8 Bibliography

Alexander, B. and Mickley, L. J. (June 2015). "Paleo-Perspectives on Potential Future Changes in the Oxidative Capacity of the Atmosphere Due to Climate Change and Anthropogenic Emissions". en. In: *Current Pollution Reports* 1.2, pp. 57–69. ISSN: 2198-6592. DOI: 10.1007/s40726-015-0006-0. URL: https://doi.org/10.1007/s40726-015-0006-0 (visited on 10/11/2023).

Allen, H. M., Crounse, J. D., et al. (2022). "H2O2 and CH3OOH (MHP) in the Remote Atmosphere: 1. Global Distribution and Regional Influences". en. In: *Journal of Geophysical Research: Atmospheres* 127.6, e2021JD035701. ISSN: 2169-8996. DOI: 10.1029/2021JD035701. URL: https://onlinelibrary.wiley.com/doi/abs/10.1029/2021JD035701 (visited on 02/21/2024).

Allen, R. J., Horowitz, L. W., et al. (Feb. 2021). "Significant climate benefits from near-term climate forcer mitigation in spite of aerosol reductions". en. In: *Environmental Research Letters* 16.3, p. 034010. ISSN: 1748-9326. DOI: 10.1088/1748-9326/abe06b. URL: https://dx.doi.org/10.1088/1748-9326/abe06b (visited on 04/15/2024).

Anklin, M. and Bales, R. C. (1997). "Recent increase in H2O2 concentration at Summit, Greenland". en. In: *Journal of Geophysical Research: Atmospheres* 102.D15, pp. 19099–19104. ISSN: 2156-2202. DOI: 10.1029/97JD01485. URL: https://onlinelibrary.wiley.com/doi/abs/10.1029/97JD01485 (visited on 01/30/2024).

Atlas, E. L. and Ridley, B. A. (1996). "The Mauna Loa Observatory Photochemistry Experiment: Introduction". en. In: *Journal of Geophysical Research: Atmospheres* 101.D9, pp. 14531–14541. ISSN: 2156-2202. DOI: 10.1029/96JD01203. URL: https://onlinelibrary.wiley.com/doi/abs/10.1029/96JD01203 (visited on 02/21/2024).

Bakker, P. et al. (Nov. 2022). "Internal climate variability and spatial temperature correlations during the past 2000 years". English. In: *Climate of the Past* 18.11, pp. 2523–2544. ISSN: 1814-9324. DOI: 10.5194/cp-18-2523-2022. URL: https://cp.copernicus.org/articles/18/2523/2022/ (visited on 01/25/2024).

Bales, R. et al. (1995). "Diel variations of H2O2 in Greenland: A discussion of the cause and effect relationship". en. In.

Balsley, B. B. and Garello, R. (1985). "The effect of El Chichón on wind variability in the troposphere, stratosphere, and mesosphere over Alaska". en. In: *Geophysical Research Letters* 12.9, pp. 581–584. ISSN: 1944-8007. DOI: 10.1029/GL012i009p00581. URL: https://onlinelibrary.wiley.com/doi/abs/10.1029/GL012i009p00581 (visited on 04/14/2024).

Banta, J. R. et al. (2008). "Spatial and temporal variability in snow accumulation at the West Antarctic Ice Sheet Divide over recent centuries". en. In: *Journal of Geophysical Research: Atmospheres* 113.D23. ISSN: 2156-2202. DOI: 10.1029/2008JD010235. URL: https://onlinelibrary.wiley.com/doi/abs/10.1029/2008JD010235 (visited on 02/03/2024).

Barth, M. C. et al. (1989). "Measurements of atmospheric gas-phase and aqueous-phase hydrogen peroxide concentrations in winter on the east coast of the United States". en. In: *Tellus B* 41B.1, pp. 61–69. ISSN: 1600-0889. DOI: 10.1111/j.1600-0889.1989.tb00125.x. URL: https://onlinelibrary.wiley.com/doi/abs/10.1111/j.1600-0889.1989.tb00125.x (visited on 02/25/2024).

Beerling, D. J. et al. (June 2011). "Enhanced chemistry-climate feedbacks in past greenhouse worlds". In: *Proceedings of the National Academy of Sciences* 108.24, pp. 9770–9775. DOI: 10.1073/pnas.1102409108. URL: https://www.pnas.org/doi/abs/10.1073/pnas.1102409108 (visited on 05/07/2024).

Berntsen, T. K. et al. (1997). "Effects of anthropogenic emissions on tropospheric ozone and its radiative forcing". en. In: *Journal of Geophysical Research: Atmospheres* 102.D23, pp. 28101–28126. ISSN: 2156-2202. DOI: 10.1029/97JD02226. URL: https://onlinelibrary.wiley.com/doi/abs/10.1029/97JD02226 (visited on 02/17/2024).

Bock, J. et al. (Oct. 2012). "Atmospheric impacts and ice core imprints of a methane pulse from clathrates". In: *Earth and Planetary Science Letters* 349-350, pp. 98–108. ISSN: 0012-821X. DOI: 10.1016/j.epsl.2012.06.052. URL: https://www.sciencedirect.com/science/article/pii/S0012821X12003445 (visited on 02/19/2024).

Bousquet, P. et al. (Oct. 2005). "Two decades of OH variability as inferred by an inversion of atmospheric transport and chemistry of methyl chloroform". English. In: *Atmospheric Chemistry and Physics* 5.10, pp. 2635–2656. ISSN: 1680-7316. DOI: 10.5194/acp-5-2635-2005. URL: https://acp.copernicus.org/articles/5/2635/2005/ (visited on 01/30/2024).

Bradshaw, J. et al. (2000). "Observed distributions of nitrogen oxides in the remote free troposphere from the Nasa Global Tropospheric Experiment Programs". en. In: *Reviews of Geophysics* 38.1, pp. 61–116. ISSN: 1944-9208. DOI: 10.1029/1999RG900015. URL: https://onlinelibrary.wiley.com/doi/abs/10.1029/1999RG900015 (visited on 02/19/2024).

Brasseur, G. P. et al. (1998). "Past and future changes in global tropospheric ozone: Impact on radiative forcing". en. In: *Geophysical Research Letters* 25.20, pp. 3807–3810. ISSN: 1944-8007. DOI: 10.1029/1998GL900013. URL: https://onlinelibrary.wiley.com/doi/abs/10.1029/1998GL900013 (visited on 02/17/2024).

Bufalini, J. J. et al. (Jan. 1979). "Hydrogen peroxide formation from the photooxidation of formaldehyde and its presence in rainwater". en. In: *Journal of Environmental Science and Health . Part A: Environmental Science and Engineering* 14.2, pp. 135–141. ISSN: 0360-1226. DOI: 10.1080/10934527909374867. URL: https://www.tandfonline.com/doi/full/10.1080/10934527909374867 (visited on 02/16/2024).

Calvert, J. G. et al. (2015). *The Mechanisms of Reactions Influencing Atmospheric Ozone*. Oxford University Press.

Chin, M. et al. (1996). "A global three-dimensional model of tropospheric sulfate". en. In: *Journal of Geophysical Research: Atmospheres* 101.D13, pp. 18667–18690. ISSN: 2156-2202. DOI: 10.1029/96JD01221. URL: https://onlinelibrary.wiley.com/doi/abs/10.1029/96JD01221 (visited on 02/19/2024).

Cohen, Y. et al. (May 2021). "Interpol-IAGOS: a new method for assessing long-term chemistry–climate simulations in the UTLS based on IAGOS data, and its application to the MOCAGE CCMI REF-C1SD simulation". English. In: *Geoscientific Model Development* 14.5, pp. 2659–2689. ISSN: 1991-959X. DOI: 10.5194/gmd-14-2659-2021. URL: https://gmd.copernicus.org/articles/14/2659/2021/ (visited on 08/07/2023).

Conley, A. J. et al. (2018). "Multimodel Surface Temperature Responses to Removal of U.S. Sulfur Dioxide Emissions". en. In: *Journal of Geophysical Research: Atmospheres*

123.5, pp. 2773–2796. ISSN: 2169-8996. DOI: 10.1002/2017JD027411. URL: https://onlinelibrary.wiley.com/doi/abs/10.1002/2017JD027411 (visited on 08/07/2023).

Crutzen, P. J. and Zimmermann, P. H. (1991). "The changing photochemistry of the troposphere". en. In: *Tellus B* 43.4, pp. 136–151. ISSN: 1600-0889. DOI: 10.1034/j.1600-0889.1991.t01-1-00012.x. URL: https://onlinelibrary.wiley.com/doi/abs/10.1034/j.1600-0889.1991.t01-1-00012.x (visited on 02/17/2024).

Danabasoglu, G. et al. (2020). "The Community Earth System Model Version 2 (CESM2)". en. In: *Journal of Advances in Modeling Earth Systems* 12.2, e2019MS001916. ISSN: 1942-2466. DOI: 10.1029/2019MS001916. URL: https://onlinelibrary.wiley.com/doi/abs/10.1029/2019MS001916 (visited on 01/05/2024).

Dentener, F. J. and Crutzen, P. J. (1993). "Reaction of N2O5 on tropospheric aerosols: Impact on the global distributions of NO x , O3, and OH". en. In: *Journal of Geophysical Research: Atmospheres* 98.D4, pp. 7149–7163. ISSN: 2156-2202. DOI: 10.1029/92JD02979. URL: https://onlinelibrary.wiley.com/doi/abs/10.1029/92JD02979 (visited on 02/19/2024).

Deser, C. et al. (Nov. 2012). "Communication of the role of natural variability in future North American climate". en. In: *Nature Climate Change* 2.11, pp. 775–779. ISSN: 1758-6798. DOI: 10.1038/nclimate1562. URL: https://www.nature.com/articles/nclimate1562 (visited on 01/25/2024).

Emmons, L. K. et al. (2020). "The Chemistry Mechanism in the Community Earth System Model Version 2 (CESM2)". en. In: *Journal of Advances in Modeling Earth Systems* 12.4, e2019MS001882. ISSN: 1942-2466. DOI: 10.1029/2019MS001882. URL: https://onlinelibrary.wiley.com/doi/abs/10.1029/2019MS001882 (visited on 10/11/2023).

Feichter, J. et al. (May 1996). "Simulation of the tropospheric sulfur cycle in a global climate model". In: *Atmospheric Environment*. Joint 8th CAGCP and 2nd IGAC Conference on Global Atmospheric Chemistry 30.10, pp. 1693–1707. ISSN: 1352-2310. DOI: 10.1016/1352-2310(95)00394-0. URL: https://www.sciencedirect.com/science/article/pii/1352231095003940 (visited on 02/19/2024).

Fiore, A. M. et al. (Nov. 2022). "Understanding recent tropospheric ozone trends in the context of large internal variability: a new perspective from chemistry-climate model ensembles". en. In: *Environmental Research: Climate* 1.2, p. 025008. ISSN: 2752-5295. DOI: 10.1088/2752-5295/ac9cc2. URL: https://dx.doi.org/10.1088/2752-5295/ac9cc2 (visited on 08/07/2023).

Frey, M. M., Stewart, R. W., et al. (2005). "Atmospheric hydroperoxides in West Antarctica: Links to stratospheric ozone and atmospheric oxidation capacity". en. In: *Journal of Geophysical Research: Atmospheres* 110.D23. ISSN: 2156-2202. DOI: 10.1029/2005JD006110. URL: https://onlinelibrary.wiley.com/doi/abs/10.1029/2005JD006110 (visited on 01/27/2024).

Frey, M. M. et al. (2006). "Climate sensitivity of the century-scale hydrogen peroxide (H2O2) record preserved in 23 ice cores from West Antarctica". en. In: *Journal of Geophysical Research: Atmospheres* 111.D21. ISSN: 2156-2202. DOI: 10.1029/2005JD006816. URL: https://onlinelibrary.wiley.com/doi/abs/10.1029/2005JD006816 (visited on 11/12/2023).

Fuglestved, J. S. et al. (1994). "Effects of reductions in stratospheric ozone on tropospheric chemistry through changes in photolysis rates". en. In: *Tellus B* 46.3, pp. 172–192. ISSN:

1600-0889. DOI: 10.1034/j.1600-0889.1992.t01-3-00001.x-i1. URL: https://onlinelibrary.wiley.com/doi/abs/10.1034/j.1600-0889.1992.t01-3-00001.x-i1 (visited on 05/16/2024).

Fuhrer, K., Neftel, A., et al. (Aug. 1993). "Continuous measurements of hydrogen peroxide, formaldehyde, calcium and ammonium concentrations along the new grip ice core from summit, Central Greenland". en. In: *Atmospheric Environment. Part A. General Topics* 27.12, pp. 1873–1880. ISSN: 09601686. DOI: 10.1016/0960-1686(93)90292-7. URL: https://linkinghub.elsevier.com/retrieve/pii/0960168693902927 (visited on 01/30/2024).

Fuhrer, K. et al. (1996). "Overview of Recent Field Experiments for the Study of the Air-Snow Transfer of H2O2 and HCHO". en. In: *Chemical Exchange Between the Atmosphere and Polar Snow*. Ed. by E. W. Wolff and R. C. Bales. Berlin, Heidelberg: Springer, pp. 307–318. ISBN: 978-3-642-61171-1. DOI: 10.1007/978-3-642-61171-1_13.

Gettelman, A. et al. (2019). "The Whole Atmosphere Community Climate Model Version 6 (WACCM6)". en. In: *Journal of Geophysical Research: Atmospheres* 124.23, pp. 12380–12403. ISSN: 2169-8996. DOI: 10.1029/2019JD030943. URL: https://onlinelibrary.wiley.com/doi/abs/10.1029/2019JD030943 (visited on 12/14/2023).

Gillett, R. W. et al. (Jan. 2000). "Formaldehyde and peroxide concentrations in Law Dome (Antarctica) firn and ice cores". en. In: *Journal of Glaciology* 46.152, pp. 15–19. ISSN: 0022-1430, 1727-5652. DOI: 10.3189/172756500781833502. URL: https://www.cambridge.org/core/journals/journal-of-glaciology/article/formaldehyde-and-peroxide-concentrations-in-law-dome-antarctica-firn-and-ice-cores/6509EE753CC644AF35F32081FDEF6435 (visited on 01/30/2024).

Grenfell, J. L. et al. (2001). "Chemistry-climate interactions in the Goddard Institute for Space Studies general circulation model: 2. New insights into modeling the preindustrial atmosphere". en. In: *Journal of Geophysical Research: Atmospheres* 106.D24, pp. 33435–33451. ISSN: 2156-2202. DOI: 10.1029/2000JD000090. URL: https://onlinelibrary.wiley.com/doi/abs/10.1029/2000JD000090 (visited on 02/17/2024).

Guo, H. et al. (Jan. 2023). "Heterogeneity and chemical reactivity of the remote troposphere defined by aircraft measurements – corrected". English. In: *Atmospheric Chemistry and Physics* 23.1, pp. 99–117. ISSN: 1680-7316. DOI: 10.5194/acp-23-99-2023. URL: https://acp.copernicus.org/articles/23/99/2023/ (visited on 01/28/2024).

Hamryszczak, Z. et al. (May 2023). "Measurement report: Hydrogen peroxide in the upper tropical troposphere over the Atlantic Ocean and western Africa during the CAFE-Africa aircraft campaign". English. In: *Atmospheric Chemistry and Physics* 23.10, pp. 5929–5943. ISSN: 1680-7316. DOI: 10.5194/acp-23-5929-2023. URL: https://acp.copernicus.org/articles/23/5929/2023/ (visited on 10/11/2023).

Hancock, S. et al. (Mar. 2023). "Changing PM $_{2.5}$ and related meteorology over India from 1950–2014: a new perspective from a chemistry-climate model ensemble". en. In: *Environmental Research: Climate* 2.1, p. 015003. ISSN: 2752-5295. DOI: 10.1088/2752-5295/acb22a. URL: https://iopscience.iop.org/article/10.1088/2752-5295/acb22a (visited on 08/07/2023).

Hartkamp, H. and Bachhausen, P. (Jan. 1987). "A method for the determination of hydrogen peroxide in air". In: *Atmospheric Environment (1967)* 21.10, pp. 2207–2213. ISSN: 0004-

6981. DOI: 10.1016/0004-6981(87)90352-0. URL: https://www.sciencedirect.com/science/article/pii/0004698187903520 (visited on 02/25/2024).

Hauglustaine, D. A. and Brasseur, G. P. (2001). "Evolution of tropospheric ozone under anthropogenic activities and associated radiative forcing of climate". en. In: *Journal of Geophysical Research: Atmospheres* 106.D23, pp. 32337–32360. ISSN: 2156-2202. DOI: 10.1029/2001JD900175. URL: https://onlinelibrary.wiley.com/doi/abs/10.1029/2001JD900175 (visited on 02/17/2024).

Heikes, B. G., Walega, J. G., et al. (1988). "Measurements of H2O2 during WATOX-86". en. In: *Global Biogeochemical Cycles* 2.1, pp. 57–61. ISSN: 1944-9224. DOI: 10.1029/GB002i001p00057. URL: https://onlinelibrary.wiley.com/doi/abs/10.1029/GB002i001p00057 (visited on 02/25/2024).

Heikes, B. G., Kok, G. L., et al. (1987). "H2O2, O3 and SO2 measurements in the lower troposphere over the eastern United States during fall". en. In: *Journal of Geophysical Research: Atmospheres* 92.D1, pp. 915–931. ISSN: 2156-2202. DOI: 10.1029/JD092iD01p00915. URL: https://onlinelibrary.wiley.com/doi/abs/10.1029/JD092iD01p00915 (visited on 02/16/2024).

Hoesly, R. M. et al. (Jan. 2018). "Historical (1750–2014) anthropogenic emissions of reactive gases and aerosols from the Community Emissions Data System (CEDS)". English. In: *Geoscientific Model Development* 11.1, pp. 369–408. ISSN: 1991-959X. DOI: 10.5194/gmd-11-369-2018. URL: https://gmd.copernicus.org/articles/11/369/2018/ (visited on 02/23/2024).

Horowitz, L. W. et al. (1998). "Export of reactive nitrogen from North America during summertime: Sensitivity to hydrocarbon chemistry". en. In: *Journal of Geophysical Research: Atmospheres* 103.D11, pp. 13451–13476. ISSN: 2156-2202. DOI: 10.1029/97JD03142. URL: https://onlinelibrary.wiley.com/doi/abs/10.1029/97JD03142 (visited on 02/19/2024).

Hough, A. M. and Derwent, R. G. (Apr. 1990). "Changes in the global concentration of tropospheric ozone due to human activities". en. In: *Nature* 344.6267, pp. 645–648. ISSN: 0028-0836, 1476-4687. DOI: 10.1038/344645a0. URL: https://www.nature.com/articles/344645a0 (visited on 02/16/2024).

Hutterli, M. A., McConnell, J. R., Chen, G., et al. (Oct. 2004). "Formaldehyde and hydrogen peroxide in air, snow and interstitial air at South Pole". In: *Atmospheric Environment*. Antarctic Atmospheric Chemistry: ISCAT 2000 38.32, pp. 5439–5450. ISSN: 1352-2310. DOI: 10.1016/j.atmosenv.2004.06.003. URL: https://www.sciencedirect.com/science/article/pii/S1352231004005175 (visited on 02/20/2024).

Hutterli, M. A., McConnell, J. R., Stewart, R. W., et al. (2001). "Impact of temperature-driven cycling of hydrogen peroxide (H2O2) between air and snow on the planetary boundary layer". en. In: *Journal of Geophysical Research: Atmospheres* 106.D14, pp. 15395–15404. ISSN: 2156-2202. DOI: 10.1029/2001JD900102. URL: https://onlinelibrary.wiley.com/doi/abs/10.1029/2001JD900102 (visited on 02/26/2024).

Inter-Tropical Convergence Zone — National Oceanic and Atmospheric Administration (2024). en. URL: https://www.noaa.gov/jetstream/tropical/convergence-zone (visited on 03/09/2024).

Jacob, P. and Klockow, D. (Nov. 1992). "Hydrogen peroxide measurements in the marine atmosphere". en. In: *Journal of Atmospheric Chemistry* 15.3, pp. 353–360. ISSN: 1573-

0662. DOI: 10.1007/BF00115404. URL: https://doi.org/10.1007/BF00115404 (visited on 02/24/2024).

Jacob, P. and Klockow, D. (Apr. 1993). "Measurements of hydrogen peroxide in Antarctic ambient air, snow and firn cores". en. In: *Fresenius' Journal of Analytical Chemistry* 346.4, pp. 429–434. ISSN: 1432-1130. DOI: 10.1007/BF00325856. URL: https://doi.org/10.1007/BF00325856 (visited on 02/24/2024).

Jacob, P., Tavares, T. M., Rocha, V. C., et al. (Jan. 1990). "Atmospheric H2O2 field measurements in a tropical environment: Bahia, Brazil". In: *Atmospheric Environment. Part A. General Topics* 24.2, pp. 377–382. ISSN: 0960-1686. DOI: 10.1016/0960-1686(90)90117-6. URL: https://www.sciencedirect.com/science/article/pii/0960168690901176 (visited on 02/24/2024).

Jacob, P. et al. (Jan. 1986). "Methodology for the determination of gaseous hydrogen peroxide in ambient air". en. In: *Fresenius' Zeitschrift für analytische Chemie* 325.4, pp. 359–364. ISSN: 1618-2650. DOI: 10.1007/BF00505460. URL: https://doi.org/10.1007/BF00505460 (visited on 02/24/2024).

Jacobi, H.-W. et al. (May 2002). "Measurements of hydrogen peroxide and formaldehyde exchange between the atmosphere and surface snow at Summit, Greenland". In: *Atmospheric Environment*. Air/Snow/Ice Interactions in the Arctic: Results from ALERT 2000 and SUMMIT 2000 36.15, pp. 2619–2628. ISSN: 1352-2310. DOI: 10.1016/S1352-2310(02)00106-1. URL: https://www.sciencedirect.com/science/article/pii/S1352231002001061 (visited on 02/26/2024).

Jain, S. et al. (June 2023). "Importance of internal variability for climate model assessment". en. In: *npj Climate and Atmospheric Science* 6.1, pp. 1–7. ISSN: 2397-3722. DOI: 10.1038/s41612-023-00389-0. URL: https://www.nature.com/articles/s41612-023-00389-0 (visited on 01/25/2024).

Kaplan, J. O. et al. (2006). "Role of methane and biogenic volatile organic compound sources in late glacial and Holocene fluctuations of atmospheric methane concentrations". en. In: *Global Biogeochemical Cycles* 20.2. ISSN: 1944-9224. DOI: 10.1029/2005GB002590. URL: https://onlinelibrary.wiley.com/doi/abs/10.1029/2005GB002590 (visited on 02/17/2024).

Karol, I. L. et al. (1995). "Radiative-photochemical modeling of the annually averaged composition and temperature of the global atmosphere during the last glacial and interglacial periods". en. In: *Journal of Geophysical Research: Atmospheres* 100.D4, pp. 7291–7301. ISSN: 2156-2202. DOI: 10.1029/94JD02385. URL: https://onlinelibrary.wiley.com/doi/abs/10.1029/94JD02385 (visited on 02/17/2024).

Kay, J. E. et al. (Aug. 2015). "The Community Earth System Model (CESM) Large Ensemble Project: A Community Resource for Studying Climate Change in the Presence of Internal Climate Variability". EN. In: *Bulletin of the American Meteorological Society* 96.8, pp. 1333–1349. ISSN: 0003-0007, 1520-0477. DOI: 10.1175/BAMS-D-13-00255.1. URL: https://journals.ametsoc.org/view/journals/bams/96/8/bams-d-13-00255.1.xml (visited on 01/25/2024).

Kelly, T. J. et al. (1985). "Measurements of peroxides in cloudwater and rain". en. In: *Journal of Geophysical Research: Atmospheres* 90.D5, pp. 7861–7871. ISSN: 2156-2202. DOI: 10.1029/JD090iD05p07861. URL: https://onlinelibrary.wiley.com/doi/abs/10.1029/JD090iD05p07861 (visited on 02/16/2024).

Kleindienst, T. E. et al. (Jan. 1988). "Comparison of techniques for measurement of ambient levels of hydrogen peroxide". In: *Environmental Science & Technology* 22.1, pp. 53–61. ISSN: 0013-936X. DOI: 10.1021/es00166a005. URL: https://doi.org/10.1021/es00166a005 (visited on 02/25/2024).

Kleinman, L. I. (1986). "Photochemical formation of peroxides in the boundary layer". en. In: *Journal of Geophysical Research: Atmospheres* 91.D10, pp. 10889–10904. ISSN: 2156-2202. DOI: 10.1029/JD091iD10p10889. URL: https://onlinelibrary.wiley.com/doi/abs/10.1029/JD091iD10p10889 (visited on 05/23/2024).

Koch, D. et al. (1999). "Tropospheric sulfur simulation and sulfate direct radiative forcing in the Goddard Institute for Space Studies general circulation model". en. In: *Journal of Geophysical Research: Atmospheres* 104.D19, pp. 23799–23822. ISSN: 2156-2202. DOI: 10.1029/1999JD900248. URL: https://onlinelibrary.wiley.com/doi/abs/10.1029/1999JD900248 (visited on 02/19/2024).

Kok, G. L. (Jan. 1980). "Measurements of hydrogen peroxide in rainwater". In: *Atmospheric Environment (1967)* 14.6, pp. 653–656. ISSN: 0004-6981. DOI: 10.1016/0004-6981(80)90048-7. URL: https://www.sciencedirect.com/science/article/pii/0004698180900487 (visited on 02/16/2024).

Kok, G. L., Heikes, B. G., et al. (Jan. 1989). "A brief survey of methods for the measurement of gas-phase hydrogen peroxide". In: *Atmospheric Environment (1967)* 23.1, p. 283. ISSN: 0004-6981. DOI: 10.1016/0004-6981(89)90124-8. URL: https://www.sciencedirect.com/science/article/pii/0004698189901248 (visited on 02/25/2024).

Kok, G. L., Holler, T. P., et al. (Sept. 1978). "Chemiluminescent method for determination of hydrogen peroxide in the ambient atmosphere". In: *Environmental Science & Technology* 12.9, pp. 1072–1076. ISSN: 0013-936X. DOI: 10.1021/es60145a010. URL: https://doi.org/10.1021/es60145a010 (visited on 02/16/2024).

Kunasek, S. A. et al. (2010). "Sulfate sources and oxidation chemistry over the past 230 years from sulfur and oxygen isotopes of sulfate in a West Antarctic ice core". en. In: *Journal of Geophysical Research: Atmospheres* 115.D18. ISSN: 2156-2202. DOI: 10.1029/2010JD013846. URL: https://onlinelibrary.wiley.com/doi/abs/10.1029/2010JD013846 (visited on 02/20/2024).

Laboratory, N. P. S. (2024). *Top 24 Strongest El Nino and La Nina Event Years by Season*. URL: https://psl.noaa.gov/enso/climaterisks/years/top24enso.html (visited on 04/14/2024).

Lamarque, J.-F., Dentener, F., et al. (Aug. 2013). "Multi-model mean nitrogen and sulfur deposition from the Atmospheric Chemistry and Climate Model Intercomparison Project (ACCMIP): evaluation of historical and projected future changes". English. In: *Atmospheric Chemistry and Physics* 13.16, pp. 7997–8018. ISSN: 1680-7316. DOI: 10.5194/acp-13-7997-2013. URL: https://acp.copernicus.org/articles/13/7997/2013/ (visited on 08/07/2023).

Lamarque, J.-F., Hess, P., et al. (2005). "Tropospheric ozone evolution between 1890 and 1990". en. In: *Journal of Geophysical Research: Atmospheres* 110.D8. ISSN: 2156-2202. DOI: 10.1029/2004JD005537. URL: https://onlinelibrary.wiley.com/doi/abs/10.1029/2004JD005537 (visited on 02/17/2024).

Lamarque, J.-F., McConnell, J. R., et al. (Feb. 2011). "Understanding the drivers for the 20th century change of hydrogen peroxide in Antarctic ice-cores: HYDROGEN PEROXIDE IN

ANTARCTIC ICE-CORES". en. In: *Geophysical Research Letters* 38.4, n/a–n/a. ISSN: 00948276. DOI: 10.1029/2010GL045992. URL: http://doi.wiley.com/10.1029/2010GL045992 (visited on 10/11/2023).

Law, K. S. and Pyle, J. A. (Jan. 1991). "Modelling the response of tropospheric trace species to changing source gas concentrations". In: *Atmospheric Environment. Part A. General Topics*. International Conference on the Generation of Oxidants Regional and Global Scales 25.9, pp. 1863–1871. ISSN: 0960-1686. DOI: 10.1016/0960-1686(91)90269-D. URL: https://www.sciencedirect.com/science/article/pii/096016869190269D (visited on 02/14/2024).

Lazrus, A. L., Kok, G. L., Gitlin, S. N., et al. (Apr. 1985). "Automated fluorimetric method for hydrogen peroxide in atmospheric precipitation". en. In: *Analytical Chemistry* 57.4, pp. 917–922. ISSN: 0003-2700, 1520-6882. DOI: 10.1021/ac00281a031. URL: https://pubs.acs.org/doi/abs/10.1021/ac00281a031 (visited on 02/25/2024).

Lazrus, A. L., Kok, G. L., Lind, J. A., et al. (Mar. 1986). "Automated fluorometric method for hydrogen peroxide in air". In: *Analytical Chemistry* 58.3, pp. 594–597. ISSN: 0003-2700. DOI: 10.1021/ac00294a024. URL: https://doi.org/10.1021/ac00294a024 (visited on 02/25/2024).

Lee, M. et al. (Jan. 2000). "Hydrogen peroxide and organic hydroperoxide in the troposphere: a review". In: *Atmospheric Environment* 34.21, pp. 3475–3494. ISSN: 1352-2310. DOI: 10.1016/S1352-2310(99)00432-X. URL: https://www.sciencedirect.com/science/article/pii/S135223109900432X (visited on 05/07/2024).

Lehner, F. and Deser, C. (May 2023). "Origin, importance, and predictive limits of internal climate variability". en. In: *Environmental Research: Climate* 2.2, p. 023001. ISSN: 2752-5295. DOI: 10.1088/2752-5295/accf30. URL: https://dx.doi.org/10.1088/2752-5295/accf30 (visited on 08/14/2023).

Lelieveld, J., Dentener, F. J., et al. (Nov. 2004). "On the role of hydroxyl radicals in the self-cleansing capacity of the troposphere". English. In: *Atmospheric Chemistry and Physics* 4.9/10, pp. 2337–2344. ISSN: 1680-7316. DOI: 10.5194/acp-4-2337-2004. URL: https://acp.copernicus.org/articles/4/2337/2004/acp-4-2337-2004.html (visited on 04/15/2024).

Lelieveld, J., Peters, W., et al. (2002). "Stability of tropospheric hydroxyl chemistry". en. In: *Journal of Geophysical Research: Atmospheres* 107.D23, ACH 17–1–ACH 17–11. ISSN: 2156-2202. DOI: 10.1029/2002JD002272. URL: https://onlinelibrary.wiley.com/doi/abs/10.1029/2002JD002272 (visited on 02/17/2024).

Lelieveld, J. and Dentener, F. J. (2000). "What controls tropospheric ozone?" en. In: *Journal of Geophysical Research: Atmospheres* 105.D3, pp. 3531–3551. ISSN: 2156-2202. DOI: 10.1029/1999JD901011. URL: https://onlinelibrary.wiley.com/doi/abs/10.1029/1999JD901011 (visited on 02/17/2024).

Levy II, H. et al. (1997). "The global impact of human activity on tropospheric ozone". en. In: *Geophysical Research Letters* 24.7, pp. 791–794. ISSN: 1944-8007. DOI: 10.1029/97GL00599. URL: https://onlinelibrary.wiley.com/doi/abs/10.1029/97GL00599 (visited on 02/17/2024).

Li, W., Li, L., Fu, R., et al. (Mar. 2011). "Changes to the North Atlantic Subtropical High and Its Role in the Intensification of Summer Rainfall Variability in the Southeastern United States". EN. In: *Journal of Climate* 24.5, pp. 1499–1506. ISSN: 0894-8755, 1520-

0442. DOI: 10.1175/2010JCLI3829.1. URL: https://journals.ametsoc.org/view/journals/clim/24/5/2010jcli3829.1.xml (visited on 04/28/2024).

Li, W., Li, L., Ting, M., et al. (Nov. 2012). "Intensification of Northern Hemisphere subtropical highs in a warming climate". en. In: *Nature Geoscience* 5.11, pp. 830–834. ISSN: 1752-0908. DOI: 10.1038/ngeo1590. URL: https://www.nature.com/articles/ngeo1590 (visited on 04/28/2024).

Liao, H. et al. (2006). "Role of climate change in global predictions of future tropospheric ozone and aerosols". en. In: *Journal of Geophysical Research: Atmospheres* 111.D12. ISSN: 2156-2202. DOI: 10.1029/2005JD006852. URL: https://onlinelibrary.wiley.com/doi/abs/10.1029/2005JD006852 (visited on 01/28/2024).

Logan, J. A. et al. (1981). "Tropospheric chemistry: A global perspective". en. In: *Journal of Geophysical Research: Oceans* 86.C8, pp. 7210–7254. ISSN: 2156-2202. DOI: 10.1029/JC086iC08p07210. URL: https://onlinelibrary.wiley.com/doi/abs/10.1029/JC086iC08p07210 (visited on 05/23/2024).

Lu, Y. and Khalil, M. A. K. (Jan. 1991). "Tropospheric OH: model calculations of spatial, temporal, and secular variations". In: *Chemosphere* 23.3, pp. 397–444. ISSN: 0045-6535. DOI: 10.1016/0045-6535(91)90194-I. URL: https://www.sciencedirect.com/science/article/pii/004565359190194I (visited on 02/16/2024).

Madronich, S. and Granier, C. (1992). "Impact of recent total ozone changes on tropospheric ozone photodissociation, hydroxyl radicals, and methane trends". en. In: *Geophysical Research Letters* 19.5, pp. 465–467. ISSN: 1944-8007. DOI: 10.1029/92GL00378. URL: https://onlinelibrary.wiley.com/doi/abs/10.1029/92GL00378 (visited on 01/25/2024).

Martinerie, P. et al. (1995). "The chemical composition of ancient atmospheres: A model study constrained by ice core data". en. In: *Journal of Geophysical Research: Atmospheres* 100.D7, pp. 14291–14304. ISSN: 2156-2202. DOI: 10.1029/95JD00826. URL: https://onlinelibrary.wiley.com/doi/abs/10.1029/95JD00826 (visited on 02/17/2024).

Masih, I. et al. (Sept. 2014). "A review of droughts on the African continent: a geospatial and long-term perspective". English. In: *Hydrology and Earth System Sciences* 18.9, pp. 3635–3649. ISSN: 1027-5606. DOI: 10.5194/hess-18-3635-2014. URL: https://hess.copernicus.org/articles/18/3635/2014/hess-18-3635-2014.html (visited on 03/31/2024).

McConnell, J. R. et al. (1997). "Physically based inversion of surface snow concentrations of H2O2 to atmospheric concentrations at South Pole". en. In: *Geophysical Research Letters* 24.4, pp. 441–444. ISSN: 1944-8007. DOI: 10.1029/97GL00183. URL: https://onlinelibrary.wiley.com/doi/abs/10.1029/97GL00183 (visited on 05/12/2024).

McKeen, S. A. et al. (1984). "On the chemistry of stratospheric SO2 from volcanic eruptions". en. In: *Journal of Geophysical Research: Atmospheres* 89.D3, pp. 4873–4881. ISSN: 2156-2202. DOI: 10.1029/JD089iD03p04873. URL: https://onlinelibrary.wiley.com/doi/abs/10.1029/JD089iD03p04873 (visited on 04/14/2024).

Michelangeli, D. V. et al. (1989). "El Chichon volcanic aerosols: Impact of radiative, thermal, and chemical perturbations". en. In: *Journal of Geophysical Research: Atmospheres* 94.D15, pp. 18429–18443. ISSN: 2156-2202. DOI: 10.1029/JD094iD15p18429. URL: https://onlinelibrary.wiley.com/doi/abs/10.1029/JD094iD15p18429 (visited on 04/14/2024).

Mickley, L. J. et al. (1999). "Radiative forcing from tropospheric ozone calculated with a unified chemistry-climate model". en. In: *Journal of Geophysical Research: Atmospheres* 104.D23, pp. 30153–30172. ISSN: 2156-2202. DOI: 10.1029/1999JD900439. URL: https://onlinelibrary.wiley.com/doi/abs/10.1029/1999JD900439 (visited on 02/17/2024).

Moller, D. (1999). "Explanation for the recent dramatic increase of H2O2 concentrations found in Greenland ice cores". In: *Atmospheric Environment* 33.

Montzka, S. A. et al. (Jan. 2011). "Small Interannual Variability of Global Atmospheric Hydroxyl". In: *Science* 331.6013, pp. 67–69. DOI: 10.1126/science.1197640. URL: https://www.science.org/doi/10.1126/science.1197640 (visited on 01/28/2024).

Murray, L. T. et al. (Apr. 2014). "Factors controlling variability in the oxidative capacity of the troposphere since the Last Glacial Maximum". English. In: *Atmospheric Chemistry and Physics* 14.7, pp. 3589–3622. ISSN: 1680-7316. DOI: 10.5194/acp-14-3589-2014. URL: https://acp.copernicus.org/articles/14/3589/2014/acp-14-3589-2014.html (visited on 02/01/2024).

Naik, V. et al. (May 2013). "Preindustrial to present-day changes in tropospheric hydroxyl radical and methane lifetime from the Atmospheric Chemistry and Climate Model Intercomparison Project (ACCMIP)". English. In: *Atmospheric Chemistry and Physics* 13.10, pp. 5277–5298. ISSN: 1680-7316. DOI: 10.5194/acp-13-5277-2013. URL: https://acp.copernicus.org/articles/13/5277/2013/ (visited on 02/17/2024).

Neftel, A. et al. (Sept. 1984). "Measurements of hydrogen peroxide in polar ice samples". en. In: *Nature* 311.5981, pp. 43–45. ISSN: 1476-4687. DOI: 10.1038/311043a0. URL: https://www.nature.com/articles/311043a0 (visited on 01/27/2024).

— (1986). "Long-term record of H2O2 in polar ice cores". en. In: *Tellus B* 38B.3-4, pp. 262–270. ISSN: 1600-0889. DOI: 10.1111/j.1600-0889.1986.tb00192.x. URL: https://onlinelibrary.wiley.com/doi/abs/10.1111/j.1600-0889.1986.tb00192.x (visited on 02/24/2024).

Neftel, A. et al. (1995). "H2O2 and HCHO in Polar Snow and Their Relation to Atmospheric Chemistry". en. In: *Ice Core Studies of Global Biogeochemical Cycles*. Ed. by R. J. Delmas. NATO ASI Series. Berlin, Heidelberg: Springer, pp. 249–264. ISBN: 978-3-642-51172-1. DOI: 10.1007/978-3-642-51172-1_14.

O'Sullivan, D. W. et al. (1999). "Distribution of hydrogen peroxide and methylhydroperoxide over the Pacific and South Atlantic Oceans". en. In: *Journal of Geophysical Research: Atmospheres* 104.D5, pp. 5635–5646. ISSN: 2156-2202. DOI: 10.1029/98JD01250. URL: https://onlinelibrary.wiley.com/doi/abs/10.1029/98JD01250 (visited on 02/21/2024).

Olson, J. R. et al. (Aug. 2012). "An analysis of fast photochemistry over high northern latitudes during spring and summer using in-situ observations from ARCTAS and TOPSE". English. In: *Atmospheric Chemistry and Physics* 12.15, pp. 6799–6825. ISSN: 1680-7316. DOI: 10.5194/acp-12-6799-2012. URL: https://acp.copernicus.org/articles/12/6799/2012/acp-12-6799-2012.html (visited on 02/21/2024).

Parrella, J. P. et al. (Aug. 2012). "Tropospheric bromine chemistry: implications for present and pre-industrial ozone and mercury". English. In: *Atmospheric Chemistry and Physics* 12.15, pp. 6723–6740. ISSN: 1680-7316. DOI: 10.5194/acp-12-6723-2012. URL: https://acp.copernicus.org/articles/12/6723/2012/acp-12-6723-2012.html (visited on 02/17/2024).

Pinto, J. P. and Khalil, M. A. K. (Jan. 1991). "The stability of tropospheric OH during ice ages, inter-glacial epochs and modern times". In: *Tellus B: Chemical and Physical Meteorology* 43.5, pp. 347–352. ISSN: null. DOI: 10.3402/tellusb.v43i5.15409. URL: https://doi.org/10.3402/tellusb.v43i5.15409 (visited on 02/16/2024).

Prather, M. J. et al. (July 2017). "Global atmospheric chemistry – which air matters". English. In: *Atmospheric Chemistry and Physics* 17.14, pp. 9081–9102. ISSN: 1680-7316. DOI: 10.5194/acp-17-9081-2017. URL: https://acp.copernicus.org/articles/17/9081/2017/acp-17-9081-2017.html (visited on 01/27/2024).

Prinn, R. G. et al. (2005). "Evidence for variability of atmospheric hydroxyl radicals over the past quarter century". en. In: *Geophysical Research Letters* 32.7. ISSN: 1944-8007. DOI: 10.1029/2004GL022228. URL: https://onlinelibrary.wiley.com/doi/abs/10.1029/2004GL022228 (visited on 01/30/2024).

Ray, J. D. et al. (1992). "The vertical distribution of atmospheric H2O2: A case study". en. In: *Journal of Geophysical Research: Atmospheres* 97.D2, pp. 2507–2517. ISSN: 2156-2202. DOI: 10.1029/91JD02056. URL: https://onlinelibrary.wiley.com/doi/abs/10.1029/91JD02056 (visited on 02/14/2024).

Ridley, B. A. et al. (1997). "Aircraft measurements made during the spring maximum of ozone over Hawaii: Peroxides, CO, O3, NOy, condensation nuclei, selected hydrocarbons, halocarbons, and alkyl nitrates between 0.5 and 9 km altitude". en. In: *Journal of Geophysical Research: Atmospheres* 102.D15, pp. 18935–18961. ISSN: 2156-2202. DOI: 10.1029/97JD01345. URL: https://onlinelibrary.wiley.com/doi/abs/10.1029/97JD01345 (visited on 02/21/2024).

Riedel, K. et al. (Jan. 2000). "Variability of tropospheric hydroperoxides at a coastal surface site in Antarctica". In: *Atmospheric Environment*. Sixth Scientific Conference of the International Global Atmospheric 34.29, pp. 5225–5234. ISSN: 1352-2310. DOI: 10.1016/S1352-2310(00)00322-8. URL: https://www.sciencedirect.com/science/article/pii/S1352231000003228 (visited on 05/12/2024).

Roelofs, G.-J. et al. (1997). "A three-dimensional chemistry/general circulation model simulation of anthropogenically derived ozone in the troposphere and its radiative climate forcing". en. In: *Journal of Geophysical Research: Atmospheres* 102.D19, pp. 23389–23401. ISSN: 2156-2202. DOI: 10.1029/97JD02210. URL: https://onlinelibrary.wiley.com/doi/abs/10.1029/97JD02210 (visited on 02/17/2024).

Schnell, J. L. and Prather, M. J. (Mar. 2017). "Co-occurrence of extremes in surface ozone, particulate matter, and temperature over eastern North America". In: *Proceedings of the National Academy of Sciences* 114.11, pp. 2854–2859. DOI: 10.1073/pnas.1614453114. URL: https://www.pnas.org/doi/10.1073/pnas.1614453114 (visited on 08/14/2023).

Schnell, R. C., Liu, S. C., et al. (June 1991). "Decrease of summer tropospheric ozone concentrations in Antarctica". en. In: *Nature* 351.6329, pp. 726–729. ISSN: 1476-4687. DOI: 10.1038/351726a0. URL: https://www.nature.com/articles/351726a0 (visited on 05/16/2024).

Seinfeld, J. and Pandis, S. (2016). *Atmospheric Chemistry and Physics: From Air Pollution to Climate Change*. 3rd ed. Wiley-Interscience.

Shindell, D. T., Faluvegi, G., Unger, N., et al. (Oct. 2006). "Simulations of preindustrial, present-day, and 2100 conditions in the NASA GISS composition and climate model G-PUCCINI". English. In: *Atmospheric Chemistry and Physics* 6.12, pp. 4427–4459. ISSN:

1680-7316. DOI: 10.5194/acp-6-4427-2006. URL: https://acp.copernicus.org/articles/6/4427/2006/ (visited on 02/17/2024).

Shindell, D., Faluvegi, G., Lacis, A., et al. (2006). "Role of tropospheric ozone increases in 20th-century climate change". en. In: *Journal of Geophysical Research: Atmospheres* 111.D8. ISSN: 2156-2202. DOI: 10.1029/2005JD006348. URL: https://onlinelibrary.wiley.com/doi/abs/10.1029/2005JD006348 (visited on 02/23/2024).

Shindell, D. T., Grenfell, J. L., et al. (2001). "Chemistry-climate interactions in the Goddard Institute for Space Studies general circulation model: 1. Tropospheric chemistry model description and evaluation". en. In: *Journal of Geophysical Research: Atmospheres* 106.D8, pp. 8047–8075. ISSN: 2156-2202. DOI: 10.1029/2000JD900704. URL: https://onlinelibrary.wiley.com/doi/abs/10.1029/2000JD900704 (visited on 02/17/2024).

Sigg, A. et al. (Apr. 1992). "Gas phase measurements of hydrogen peroxide in Greenland and their meaning for the interpretation of H2O2 records in ice cores". en. In: *Journal of Atmospheric Chemistry* 14.1, pp. 223–232. ISSN: 1573-0662. DOI: 10.1007/BF00115235. URL: https://doi.org/10.1007/BF00115235 (visited on 02/24/2024).

Sigg, A. and Neftel, A. (Jan. 1988). "Seasonal Variations in Hydrogen Peroxide in Polar Ice Cores". en. In: *Annals of Glaciology* 10, pp. 157–162. ISSN: 0260-3055, 1727-5644. DOI: 10.3189/S0260305500004353. URL: https://www.cambridge.org/core/journals/annals-of-glaciology/article/seasonal-variations-in-hydrogen-peroxide-in-polar-ice-cores/2B824B387A565B45600FC8A402CCE67A (visited on 01/25/2024).

— (June 1991). "Evidence for a 50% increase in H202 over the past 200 years from a Greenland ice core". en. In: *Nature* 351.6327, pp. 557–559. ISSN: 1476-4687. DOI: 10.1038/351557a0. URL: https://www.nature.com/articles/351557a0 (visited on 02/14/2024).

Singh, H. B. et al. (Oct. 1999). "SONEX airborne mission and coordinated POLINAT-2 activity: Overview and accomplishments". en. In: *Geophysical Research Letters* 26.20, pp. 3053–3056. ISSN: 0094-8276, 1944-8007. DOI: 10.1029/1999GL900588. URL: https://agupubs.onlinelibrary.wiley.com/doi/10.1029/1999GL900588 (visited on 02/23/2024).

Slemr, F. et al. (1986). "Measurement of gas phase hydrogen peroxide in air by tunable diode laser absorption spectroscopy". en. In: *Journal of Geophysical Research: Atmospheres* 91.D5, pp. 5371–5378. ISSN: 2156-2202. DOI: 10.1029/JD091iD05p05371. URL: https://onlinelibrary.wiley.com/doi/abs/10.1029/JD091iD05p05371 (visited on 02/25/2024).

Sofen, E. D., Alexander, B., Steig, E. J., et al. (June 2014). "WAIS Divide ice core suggests sustained changes in the atmospheric formation pathways of sulfate and nitrate since the 19th century in the extratropical Southern Hemisphere". English. In: *Atmospheric Chemistry and Physics* 14.11, pp. 5749–5769. ISSN: 1680-7316. DOI: 10.5194/acp-14-5749-2014. URL: https://acp.copernicus.org/articles/14/5749/2014/acp-14-5749-2014.html (visited on 02/24/2024).

Sofen, E. D. et al. (Apr. 2011). "The impact of anthropogenic emissions on atmospheric sulfate production pathways, oxidants, and ice core Δ^{17}O(SO_4^{2}–)". English. In: *Atmospheric Chemistry and Physics* 11.7, pp. 3565–3578. ISSN: 1680-7316. DOI: 10.5194/acp-11-3565-2011. URL: https://acp.copernicus.org/articles/11/3565/2011/acp-11-3565-2011.html (visited on 02/01/2024).

Spivakovsky, C. M. et al. (1990). "Tropospheric OH in a three-dimensional chemical tracer model: An assessment based on observations of CH3CCl3". en. In: *Journal of Geophysical Research: Atmospheres* 95.D11, pp. 18441–18471. ISSN: 2156-2202. DOI: 10.1029/JD095iD11p18441. URL: https://onlinelibrary.wiley.com/doi/abs/10.1029/JD095iD11p18441 (visited on 02/19/2024).

Staffelbach, T., Neftel, A., et al. (Feb. 1991). "A record of the atmospheric methane sink from formaldehyde in polar ice cores". en. In: *Nature* 349.6310, pp. 603–605. ISSN: 1476-4687. DOI: 10.1038/349603a0. URL: https://www.nature.com/articles/349603a0 (visited on 02/17/2024).

Staffelbach, T. A., Kok, G. L., et al. (1996). "Comparison of hydroperoxide measurements made during the Mauna Loa Observatory Photochemistry Experiment 2". en. In: *Journal of Geophysical Research: Atmospheres* 101.D9, pp. 14729–14739. ISSN: 2156-2202. DOI: 10.1029/95JD02197. URL: https://onlinelibrary.wiley.com/doi/abs/10.1029/95JD02197 (visited on 02/25/2024).

Stevenson, D. S. et al. (Nov. 2020). "Trends in global tropospheric hydroxyl radical and methane lifetime since 1850 from AerChemMIP". English. In: *Atmospheric Chemistry and Physics* 20.21, pp. 12905–12920. ISSN: 1680-7316. DOI: 10.5194/acp-20-12905-2020. URL: https://acp.copernicus.org/articles/20/12905/2020/ (visited on 04/15/2024).

Stolarski, R. S. et al. (1991). "Total Ozone trends deduced from Nimbus 7 Toms data". en. In: *Geophysical Research Letters* 18.6, pp. 1015–1018. ISSN: 1944-8007. DOI: 10.1029/91GL01302. URL: https://onlinelibrary.wiley.com/doi/abs/10.1029/91GL01302 (visited on 01/25/2024).

Stolzenburg, D. et al. (June 2020). "Enhanced growth rate of atmospheric particles from sulfuric acid". English. In: *Atmospheric Chemistry and Physics* 20.12, pp. 7359–7372. ISSN: 1680-7316. DOI: 10.5194/acp-20-7359-2020. URL: https://acp.copernicus.org/articles/20/7359/2020/ (visited on 04/14/2024).

Tarasick, D. et al. (Oct. 2019). "Tropospheric Ozone Assessment Report: Tropospheric ozone from 1877 to 2016, observed levels, trends and uncertainties". In: *Elementa: Science of the Anthropocene* 7. Ed. by D. Helmig and A. Lewis, p. 39. ISSN: 2325-1026. DOI: 10.1525/elementa.376. URL: https://doi.org/10.1525/elementa.376 (visited on 05/07/2024).

The Intergovernmental Panel on Climate Change (2024). *Atmospheric Lifetimes and Time-Scales*. URL: https://archive.ipcc.ch/ipccreports/tar/wg1/133.htm (visited on 05/23/2024).

Thompson, A. M., Chappellaz, J. A., et al. (Jan. 1993). "The atmospheric CH4 increase since the Last Glacial Maximum". In: *Tellus B: Chemical and Physical Meteorology* 45.3, pp. 242–257. ISSN: null. DOI: 10.3402/tellusb.v45i3.15727. URL: https://doi.org/10.3402/tellusb.v45i3.15727 (visited on 10/11/2023).

Thompson, A. M. (May 1992). "The Oxidizing Capacity of the Earth's Atmosphere: Probable Past and Future Changes". en. In: *Science* 256.5060, pp. 1157–1165. ISSN: 0036-8075, 1095-9203. DOI: 10.1126/science.256.5060.1157. URL: https://www.science.org/doi/10.1126/science.256.5060.1157 (visited on 10/18/2023).

Thompson, A. M. et al. (1989). "Sensitivity of tropospheric hydrogen peroxide to global chemical and climate change". en. In: *Geophysical Research Letters* 16.1, pp. 53–56. ISSN:

1944-8007. DOI: 10.1029/GL016i001p00053. URL: https://onlinelibrary.wiley.com/doi/abs/10.1029/GL016i001p00053 (visited on 10/11/2023).

Thompson, A. M. et al. (Jan. 1991). "Perturbations to tropospheric oxidants, 1985–2035: 2. Calculations of hydrogen peroxide in chemically coherent regions". In: *Atmospheric Environment. Part A. General Topics*. International Conference on the Generation of Oxidants Regional and Global Scales 25.9, pp. 1837–1850. ISSN: 0960-1686. DOI: 10.1016/0960-1686(91)90267-B. URL: https://www.sciencedirect.com/science/article/pii/096016869190267B (visited on 11/06/2023).

Tilmes, S. et al. (May 2015). "Description and evaluation of tropospheric chemistry and aerosols in the Community Earth System Model (CESM1.2)". English. In: *Geoscientific Model Development* 8.5, pp. 1395–1426. ISSN: 1991-959X. DOI: 10.5194/gmd-8-1395-2015. URL: https://gmd.copernicus.org/articles/8/1395/2015/gmd-8-1395-2015.html (visited on 02/21/2024).

Turner, A. J. et al. (Sept. 2018). "Modulation of hydroxyl variability by ENSO in the absence of external forcing". In: *Proceedings of the National Academy of Sciences* 115.36, pp. 8931–8936. DOI: 10.1073/pnas.1807532115. URL: https://www.pnas.org/doi/full/10.1073/pnas.1807532115 (visited on 04/14/2024).

Turner, J. (2004). "The El Niño–southern oscillation and Antarctica". en. In: *International Journal of Climatology* 24.1, pp. 1–31. ISSN: 1097-0088. DOI: 10.1002/joc.965. URL: https://onlinelibrary.wiley.com/doi/abs/10.1002/joc.965 (visited on 03/01/2024).

Valdes, P. J. et al. (2005). "The ice age methane budget". en. In: *Geophysical Research Letters* 32.2. ISSN: 1944-8007. DOI: 10.1029/2004GL021004. URL: https://onlinelibrary.wiley.com/doi/abs/10.1029/2004GL021004 (visited on 02/17/2024).

Volz, A. and Kley, D. (Mar. 1988). "Evaluation of the Montsouris series of ozone measurements made in the nineteenth century". en. In: *Nature* 332.6161, pp. 240–242. ISSN: 1476-4687. DOI: 10.1038/332240a0. URL: https://www.nature.com/articles/332240a0 (visited on 02/14/2024).

Wang, Y. and Jacob, D. J. (1998). "Anthropogenic forcing on tropospheric ozone and OH since preindustrial times". en. In: *Journal of Geophysical Research: Atmospheres* 103.D23, pp. 31123–31135. ISSN: 2156-2202. DOI: 10.1029/1998JD100004. URL: https://onlinelibrary.wiley.com/doi/abs/10.1029/1998JD100004 (visited on 02/14/2024).

Wang, Y., Ridley, B., et al. (2003). "Springtime photochemistry at northern mid and high latitudes". en. In: *Journal of Geophysical Research: Atmospheres* 108.D4. ISSN: 2156-2202. DOI: 10.1029/2002JD002227. URL: https://onlinelibrary.wiley.com/doi/abs/10.1029/2002JD002227 (visited on 02/21/2024).

Wang, Y. et al. (1998). "Global simulation of tropospheric O3-NO x -hydrocarbon chemistry: 2. Model evaluation and global ozone budget". en. In: *Journal of Geophysical Research: Atmospheres* 103.D9, pp. 10727–10755. ISSN: 2156-2202. DOI: 10.1029/98JD00157. URL: https://onlinelibrary.wiley.com/doi/abs/10.1029/98JD00157 (visited on 02/18/2024).

Westervelt, D. M. et al. (Mar. 2020). "Local and remote mean and extreme temperature response to regional aerosol emissions reductions". English. In: *Atmospheric Chemistry and Physics* 20.5, pp. 3009–3027. ISSN: 1680-7316. DOI: 10.5194/acp-20-3009-2020. URL: https://acp.copernicus.org/articles/20/3009/2020/ (visited on 08/07/2023).

Wu, S. et al. (2008). "Effects of 2000–2050 changes in climate and emissions on global tropospheric ozone and the policy-relevant background surface ozone in the United States". en. In: *Journal of Geophysical Research: Atmospheres* 113.D18. ISSN: 2156-2202. DOI: 10.1029/2007JD009639. URL: https://onlinelibrary.wiley.com/doi/abs/10.1029/2007JD009639 (visited on 01/30/2024).

Young, P. J. et al. (Feb. 2013). "Pre-industrial to end 21st century projections of tropospheric ozone from the Atmospheric Chemistry and Climate Model Intercomparison Project (ACCMIP)". English. In: *Atmospheric Chemistry and Physics* 13.4, pp. 2063–2090. ISSN: 1680-7316. DOI: 10.5194/acp-13-2063-2013. URL: https://acp.copernicus.org/articles/13/2063/2013/ (visited on 02/14/2024).

Zhai, S. et al. (2021). "Anthropogenic Impacts on Tropospheric Reactive Chlorine Since the Preindustrial". en. In: *Geophysical Research Letters* 48.14, e2021GL093808. ISSN: 1944-8007. DOI: 10.1029/2021GL093808. URL: https://onlinelibrary.wiley.com/doi/abs/10.1029/2021GL093808 (visited on 04/14/2024).

Zhang, Q. et al. (June 2021). "Atmospheric nitrogen deposition: A review of quantification methods and its spatial pattern derived from the global monitoring networks". en. In: *Ecotoxicology and Environmental Safety* 216, p. 112180. ISSN: 0147-6513. DOI: 10.1016/j.ecoenv.2021.112180. URL: https://www.sciencedirect.com/science/article/pii/S0147651321002918 (visited on 08/07/2023).

Zhao, Y., Saunois, M., et al. (Nov. 2020). "On the role of trend and variability in the hydroxyl radical (OH) in the global methane budget". English. In: *Atmospheric Chemistry and Physics* 20.21, pp. 13011–13022. ISSN: 1680-7316. DOI: 10.5194/acp-20-13011-2020. URL: https://acp.copernicus.org/articles/20/13011/2020/ (visited on 02/28/2024).

Zhao, Z. and Wang, Y. (Dec. 2017). "Influence of the West Pacific subtropical high on surface ozone daily variability in summertime over eastern China". In: *Atmospheric Environment* 170, pp. 197–204. ISSN: 1352-2310. DOI: 10.1016/j.atmosenv.2017.09.024. URL: https://www.sciencedirect.com/science/article/pii/S1352231017306155 (visited on 04/28/2024).

Zheng, Z. et al. (2023). "Automated Machine Learning to Evaluate the Information Content of Tropospheric Trace Gas Columns for Fine Particle Estimates Over India: A Modeling Testbed". en. In: *Journal of Advances in Modeling Earth Systems* 15.3, e2022MS003099. ISSN: 1942-2466. DOI: 10.1029/2022MS003099. URL: https://onlinelibrary.wiley.com/doi/abs/10.1029/2022MS003099 (visited on 08/14/2023).